Quantum maps with space extent:
a paradigm for lattice quantum walks

Daniel K. Wójcik

Nencki Institute of Experimental Biology, Department of Neurophysiology,
3 Pasteur Str., 02-093 Warsaw, Poland
d.wojcik@nencki.gov.pl

Classical Multibaker Maps are deterministic models of classical random walks. Quantum Multibaker Maps are their quantum versions. As such, they can be naturally considered quantum random walks. In this review we discuss the construction and properties of quantum multibaker maps and related, more general models, in the context of the recent results in dynamical systems approach to nonequilibrium statistical mechanics. Properties of other models of quantum walks are also discussed.

Keywords: multibaker maps; transport; nonequilibrium statistical mechanics; quantum walks

1. Introduction

Dynamical systems theory from its conception found most applications in low-dimensional mechanical systems [40,51,154]. Since the reduction of Lorentz gas on regular lattice to a billiard problem [27,181,211] methods of chaos theory have pervaded nonequilibrium statistical mechanics. In the course of last fifteen years we have seen growth of interest in the connections between the two fields as new results were discovered [46,74,121,174,185].

The impetus came from two directions. One was from molecular dynamics simulations of transport processes, where one has to deal with the problem of particle heating. To overcome it a number of dynamical thermostatting mechanisms were invented [57,102,120,146,168]. The thermostats are implemented through changes in the equations of motion which are done in such a way as to eliminate the heat, for instance by constraining the total or kinetic energy, while at the same time producing results consistent with the experiments. In certain cases it was possible to show that in the limit of small driving fields original dynamics is recovered and the numerically obtained transport coefficients are equivalent to those given by the usual linear response theory [57,102].

The thermostatted equations of motion are typically dissipative and chaotic [66]. It turns out that the transport coefficients of thermostatted systems can be connected

2   *Daniel K. Wójcik*

to their Lyapunov spectrum. For instance, electrical conductivity σ of Gaussian thermostatted 2D Lorentz gas is given by $\sigma = -k_B T \langle \lambda_+ + \lambda_- \rangle / E^2$, where E is the driving field, T is the ambient temperature, $\lambda_\pm$ are the Lyapunov exponents of the system [30,31].

Another remarkable outcome of the studies of thermostatted systems is the fluctuation theorem [56,65,66], which quantifies the probability of observing states deviating from what is expected from nonequilibrium thermodynamics. An example of such state is provided by a charged particle bouncing from a scatterer in the Lorentz gas against the direction of the driving field. Since the original formulation of the theorem a number of related results has appeared [8,58,59,112,130,133,139]. The study of various fluctuation theorems as well as of related [38] free energy relations [28,37,110,111,166], both theoretical and experimental [35,48,67,135,202], is flourishing. While most of the results in this field were obtained for molecular type systems, often low dimensional, there are attempts to understand the role of dynamical instabilities as expressed by the Lyapunov exponents and of different "dynamical ensembles" in the description of spatiotemporal systems, such as fluids [64,68].

Second approach which turned out very productive in connecting dynamical systems theory with nonequilibrium statistical mechanics was through transient chaos and the study of escape processes [13,20,114,115,190]. Here, formulas for transport coefficients were found in terms of Lyapunov exponents and Kolmogorov-Sinai entropy on the repeller [83]. The amazing discovery of fractal character of the microscopic hydrodynamic modes of diffusion [47,72,80,90,187] shed new light on the properties of entropy production in nonequilibrium systems. The incomplete van Hove functions [72,80,196] probing the diffusion processes at different wave numbers k are fractal functions of Takagi type [212] whose fractal dimension $D_H(k) = 1 + \frac{D}{\lambda}k^2 + O(k^4)$ is given in terms of the diffusion coefficient D and the largest Lyapunov exponent λ [80,90].

Conceptually important development concerned understanding and extraction of Pollicott-Ruelle resonances [158,159,171,172,173] which determine the exponential decay of certain correlation functions in time-reversible hyperbolic systems. With this concept it was possible to describe macroscopic breaking of time-reversal for microscopically reversible systems [49,69,74,76,78,119,203].

Most of these phenomena are the results of nonlinear and nonintegrable character of typical spatially extended classical systems. The linearity of quantum mechanics makes one wonder if any of the remarkable results obtained for the classical systems survive in the quantum regime? While quantum fractals can be constructed [15,207] they are not expected as nonequilibrium steady states of quantum nonequilibrium systems.

It turns out that the importance of Pollicott-Ruelle resonances extends to quantum mechanics where they rule the relaxation of the quantum correlation functions and survival probability in the semiclassical regime [1,75,78,85,86,87,137,143,155,204]. This regime is sometimes called the "Lyapunov regime" [106,107] because the leading resonance is often given by the largest Lyapunov exponent, especially in simple systems with uniform stretching, such as baker map. Different regions of relaxation have

recently been studied in the connection with the so-called problem of Loschmidt echoes or fidelity decay [39,92,106,107,109,157,162,205]. Here the main objective was the quantification of quantum instability against small perturbations of the system under study.

In many-body quantum systems with continuous spectra, such as spin-boson [82] or other systems coupled to infinite heat reservoirs [108], or other many-body systems [55,161], the quantum analogues of Pollicott-Ruelle resonances are the poles of analytic continuation of von Neumann operator. There is also a huge body of literature devoted to the applications of random matrix theory to mesoscopic systems [14,52,94,104] for quantum dots [4], quantum wires [14] and for antidot lattices [61]. However, most of these works are not much concerned with the connections to classical instability and rather explore the random properties of spectra of the disordered systems.

Important model systems for which many of the classical results were tested are classical multibaker maps [69,74]. They are area-preserving deterministic models of one-dimensional random walks. We briefly review their construction and properties in Section 2. To obtain a simple, intuitive model, useful for the studies of the signatures of classical chaos in the quantum transport we have quantized the classical multibaker map [208,209,210]. We review the construction of the obtained model which we called quantum multibaker map, in Section 3. A more general framework of quantum maps with space extent, which we call quantum multiplexer maps, is also presented there. Properties of several versions of quantum multiplexer maps are discussed in Section 4. As quantizations of deterministic models of random walks on a lattice, quantum multibaker maps can be considered a paradigm for quantum random walks. We review some of the recent studies of quantum walks conducted in the context of quantum information theory in Section 5. We summarize this review with some open questions and perspectives in Section 6.

2. Classical multibaker maps

Classical multibaker maps were introduced into statistical mechanics by Pierre Gaspard [69] as translationally invariant extensions of Elskens-Kapral model of chemical reactions [53]. Since then, many variants of the model were considered, the simplest of which, dyadic multibaker map [187], was in fact considered already in 1930's by Eberhard Hopf [103] as an example of a mixing system with infinite measure.

The model can be introduced in several different ways. One approach is to take the suspension of the flow in a periodic, quasi one-dimensional Lorentz channel [72,77]. That is, consider the separation of the flow into three components: a volume preserving mapping in Birkhoff coordinates [17] on the circular scatterer, a mapping between consecutive scattering times, and a function describing jumps on a lattice [72,74]. If we disregard the precise information about scattering times and approximate the nonlinear Poincare-Birkhoff map by a piecewise linear baker map, the simplified suspension flow becomes dyadic multibaker map.

4   *Daniel K. Wójcik*

Fig. 1.   Quasi one-dimensional Lorentz channel. Simplification of dynamics of a particle in the channel leads to the classical multibaker map.

An alternative derivation comes from the considerations of one-dimensional random walks on a lattice. Imagine a particle jumping on a lattice and assume the mechanism of jump is deterministic. In every jump the particle can go right or left to one of its nearest neighbors. If the only variable determining its state is the position on the lattice and we require translational invariance of the dynamics then the only type of motion possible is shift in one direction. To allow for less trivial dynamics we must assume that the particle has some internal degrees of freedom which determine the direction of motion and which are altered during the jump in a deterministic way (e.g. due to an external field or coupling with lattice degrees of freedom). If we want the resulting motion to be random this requires a degree of chaoticity. A simple possibility is to model the internal state of the particle by a point in a compact phase space and decompose the dynamics into a jump to the neighboring site followed by a local transformation of the internal state. Modelling the internal dynamics by the classical baker map, with the appropriate identification of the states going left or right, the full system evolves according to the classical multibaker map. The advantage of using baker map over other local chaotic maps is the immediate isomorphism between trajectories of the multibaker map and the standard one-dimensional random walk on the lattice.

The need for considering such models stems from considerations of the Brownian motion. Since the erraticity of the Brownian particle is due to a large number of *deterministic* collisions with fluid molecules one may wonder if there are traces of this determinism to be found in macroscopic description of the model[79]. This is easiest to answer in the simplified Brownian motion, one-dimensional random walk, which in turn can be modeled deterministically by a multibaker map.

The simplest dyadic version of multibaker map[103,187] is defined by

$$M(n,x,y) = \begin{cases} (n+1, 2x, y/2), & \text{for } 0 \le x < 1/2, \\ (n-1, 2x-1, (1+y)/2), & \text{for } 1/2 \le x < 1. \end{cases} \qquad (1)$$

It can be written as a composition of two maps $M = B \circ T$, where T moves the phase point to a neighboring cell

$$T(n,x,y) = \begin{cases} (n+1, x, y), & \text{for } 0 \le x < 1/2, \\ (n-1, x, y), & \text{for } 1/2 \le x < 1, \end{cases}$$

and the baker map, B, which acts locally in every cell n

$$B(n,x,y) = \begin{cases} (n, 2x, y/2), & \text{for } 0 \le x < 1/2, \\ (n, 2x-1, (1+y)/2), & \text{for } 1/2 \le x < 1. \end{cases}$$

Thus it is a two-dimensional lattice system where the phase space at each lattice site is a square (or a torus). The dynamics is a combination of transport of the phase space densities to neighboring cells, which models the free flight, followed by a local baker map evolution within a square, modeling a collision with a fixed scatterer. The multibaker map is a time-reversible, measure preserving, chaotic (Bernoulli) transformation.

The complete solvability of this model and its variants makes them ideal for testing and deriving connections between macroscopic transport properties and the characteristics of dynamical instability. Thus exact Pollicott-Ruelle resonances were obtained for these maps[69,187] as well as the escape rate, Lyapunov exponent, KS entropy and the information dimension. The escape-rate formula[83]

$$D = \lim_{L \to \infty} \left(\frac{L}{\pi} \right)^2 [\lambda - h_{KS}] \tag{2}$$

connecting the diffusion coefficient D with the Lyapunov exponent λ and the KS entropy h_{KS} on the repeller was verified and the PR resonances were shown to be approximated well by the spectrum of macroscopic diffusion equation[69,74].

Generalized eigenstates of the Frobenius-Perron operator for multibaker map are given by fractal de Rham functions[71] just like for an associated one-dimensional maps[70,99,100]. This fractality shows up as well in the cumulative functions describing the stationary states[47,186,187]. The singularity of the invariant measures describing steady states with respect to the Liouville measure was claimed to be the reason for positivity of entropy production in steady states[73,76,88,89,189]. A different approach to entropy production, through the Kullback information loss for coarse-grained phase space densities, was intensely studied by Breymann, Matyas, Tél, and Vollmer[23,24,198,199,201] as reviewed in[191,197,200]. The applicability of these concepts to nonequilibrium statistical mechanics of more general systems has been a matter of some controversy[36,84,169,193]. In our opinion, as long as extending these results for fluid systems, where one will be able to compare the usual thermodynamic formulas with the Gaspard-Gilbert-Dorfman entropy production, seems viable[a], one should wait for further developments. Definitely, the studies of entropy production from dynamical systems perspective where one of the important topics in nonequilibrium statistical mechanics explored with the help of multibaker models.

Multibaker maps are very flexible models. Several hamiltonian (area-preserving) versions were used[69,187,188,189], mostly in the framework of the escape rate theory, dissipative variants were considered[23,88,140,141,170,192,198,201] for testing the results of thermostatted approach to nonequilibrium thermodynamics. These models were used to model diffusion in usual[69,187] and biased[88] random walks, diffusion-reaction processes[81], diffusion in the Lorentz gas in the presence of electric field[188,189,192], to test global and local fluctuation theorems for steady states[170], thermodynamic cross effects[140,141,201] as well as shear flow and viscous heating[142]. For detailed

---

[a]J. R. Dorfman, private communication.

reviews of the properties of different variants of classical multibaker maps and associated models we recommend the monographs by Pierre Gaspard[74] and by Jürgen Vollmer[197] as well as the reviews by Tel, Vollmer and Breymann[191,200].

3. Quantum maps with space extent

Quantum multibaker maps[208,209,210] were introduced as quantizations of the Tasaki-Gaspard classical multibaker model[187]. They are simple models of quantum particle jumping on a lattice. Depending on its internal state the particle jumps one step left or one step right. This is interpreted dynamically as resulting from scattering on an obstacle. The scattering of the particle is modeled by the quantum baker map. Quantum baker maps form a two-parameter family parametrized by two phases[44,177]. In the construction of quantum multibaker map these phases can be set identical at every lattice site which leads to a translationally invariant model. It is characterized by coherent transport of probability amplitudes left and right resulting in ballistic motion[209,210]. Choosing the two phases at every lattice site randomly from some prescribed distribution one can obtain a disordered model characterized by localization of the wave functions[208]. Therefore, the quantum multibaker maps in their original formulation are a rich family of models parametrized by the number of internal quantum states N, which plays the role of the inverse Planck constant, by the length of the chain L, and by the distribution of phases. The large N limit is the semiclassical limit in which we recover the classical properties. Large L limit corresponds to thermodynamic limit.

These maps can be further generalized to more dimensions, other local operators can be used instead of quantum bakers, and the range of interaction can be longer. We call these generalized models *quantum multiplexer maps*. Appropriate choice of boundary conditions allows one to study closed and open systems as well as stationary states in systems connected to particle reservoirs. In this section we review the construction and properties of quantum multibaker maps and some of these generalizations.

3.1. *Quantum baker map*

Quantization of an area-preserving map consists of specification of the Hilbert space (prequantization) and constructing a unitary operator acting on that space. Construction of Hilbert spaces associated with the two-torus is by now well-understood[11,22,41,42,44,97,176]. Assume the fundamental square has sides of length a in position and b in momentum. Then periodicity in position representation $\Psi(q + a) = e^{i\alpha_q}\Psi(q)$ requires that momentum representation takes non-zero values only at a discrete set of momenta $p_k = \frac{h}{a}(k + \varphi_p)$, where $\alpha_q = 2\pi\varphi_p$. Similarly, periodicity in momentum representation $\tilde{\Psi}(p+b) = e^{i\alpha_p}\tilde{\Psi}(p)$ requires $q_l = \frac{h}{b}(l+\varphi_q)$, where $\alpha_p = -2\pi\varphi_q$. Here $\varphi_q, \varphi_p \in [0,1)$ are phases parametrizing quantization and define the boundary conditions on the torus. Since a must be an integer multiple of h/b one obtains Bohr-Sommerfeld quantization condition $2\pi\hbar N = ab$. Choosing

units so that $a = b = 1$ one arrives at a relation between the Planck constant and the dimension of Hilbert space $h = 1/N$.

Since the space of double periodic wave functions is N-dimensional Hilbert space we represent wave functions by N-dimensional vectors. The space and momentum representations are connected by a discrete Fourier transform $\langle p_k | q_l \rangle = [G_N(\varphi_q, \varphi_p)]_{k,l} := N^{-1/2} \exp(-i2\pi N p_k q_l)$. The discrete positions and momenta are $q_l = (l + \varphi_q)/N$, $p_k = (k + \varphi_p)/N$, respectively; $l, k = 0, \dots N-1$. The structure of the classical baker map requires us to take N even. We label the quantum states in coordinate space by $j = 0, 1, \dots, N - 1$. We call the first $N/2$ position states $j = 0, \dots N/2 - 1$ the "left" states, with collective wave function, Ψ_L, while the remaining position states, $j = N/2, \dots, N - 1$ are called the "right" states, with wave function Ψ_R.

Equipped with the Hilbert space we look for a family of unitary propagators parametrized by $N = 1/h$ which approach the classical map in semi-classical limit. There is no general quantization procedure for area-preserving maps but in cases where a generating function exists one can use it to construct such a family [10,41]. Such a quantization of baker map using a mixed generating function was performed by Saraceno and Voros [177]. The quantum baker operator [11,44,176,177] is given by a combination of two operations. The first operation transforms the $N/2$ "left" states into momentum states labeled $k = 0, 1, \dots, N/2 - 1$, which we call "bottom" momentum states, by means of the $N/2 \times N/2$ Fourier transform matrix $G_{N/2}(\varphi_q, \varphi_p)$. The "right" coordinate states are transformed to "top" momentum states in the same way. Thus the N spatial states are transformed into N momentum states in a way that mimics the classical baker's map. One has to now express the N new states in coordinate representation by means of the inverse Fourier transform G_N^{-1}. Thus the quantum baker transformation, B, in the position representation, is given by the unitary matrix

$$B := G_N^{-1}(\varphi_q, \varphi_p) \begin{bmatrix} G_{N/2}(\varphi_q, \varphi_p) & 0 \\ 0 & G_{N/2}(\varphi_q, \varphi_p) \end{bmatrix}. \tag{3}$$

3.2. *Quantum multibaker maps*

Quantum multibaker map is a model of quantum particle transport on the lattice. Thus the Hilbert space of the model is the tensor product of the lattice Hilbert space H_L with the Hilbert space of internal dynamics H_I. For the quantum baker map H_I is the Hilbert space for the torus described above. For one-dimensional model on a lattice of length L the Hilbert space of the model is $\mathbb{C}^L \otimes \mathbb{C}^N$, where $N = 1/h$ is the number of internal states.

We denote the basis states by $|n, \varepsilon, i\rangle \equiv |n\rangle \otimes |\varepsilon\rangle \otimes |i\rangle$, where n is the lattice site, $\varepsilon = \pm 1$ denotes these states which will be transported to site $n + \varepsilon$ in one time step, and $i = 0, \dots, N/2 - 1$ enumerates the states corresponding to a given half of the classical square in position representation. Thus the Hilbert space of the system is a simple sum of spaces $H_\varepsilon(n)$ span by the states $|n, \varepsilon, i\rangle$ which are moved in one

8   *Daniel K. Wójcik*

time unit from lattice site n to site $n + \varepsilon$. Then the general wave function for the multibaker chain can be written as

$$|\Psi\rangle = \sum_n \sum_\varepsilon \sum_i \Psi_{n,\varepsilon,i} |n, \varepsilon, i\rangle \equiv \sum_n \sum_\varepsilon |n\rangle \otimes |\varepsilon\rangle \otimes |\Psi_\varepsilon(n)\rangle, \tag{4}$$

where $|\Psi_\varepsilon(n)\rangle$ is $N/2$ dimensional vector describing the internal states of the particle at site n which will move in one time-step to site $n + \varepsilon$. The inner product takes form

$$\langle\Phi|\Psi\rangle = \sum_n \sum_\varepsilon \sum_i \Phi^*_{n,\varepsilon,i} \Psi_{n,\varepsilon,i} \equiv \sum_n \sum_\varepsilon \langle\Phi_\varepsilon(n)|\Psi_\varepsilon(n)\rangle. \tag{5}$$

The dynamics is composed of two operations. First, depending on the internal state, the particle moves one step left or right so that $\Psi_\varepsilon(n) \to \Psi_\varepsilon(n + \varepsilon)$. Then its internal state is randomized according to local quantum baker dynamics. The first operation models the free flight in the Lorentz gas while the local randomization of states resulting from an application of a quantum baker map models scattering on an obstacle. The result, in the position representation[b], is given by

$$\begin{bmatrix} \Psi_+(n, t+1) \\ \Psi_-(n, t+1) \end{bmatrix} = B(n) \cdot \begin{bmatrix} \Psi_+(n-1, t) \\ \Psi_-(n+1, t) \end{bmatrix}, \tag{6}$$

where

$$B(n) = G_N^{-1}(n) \cdot \begin{bmatrix} G_{N/2}(n) & 0 \\ 0 & G_{N/2}(n) \end{bmatrix}, \tag{7}$$

and $G_N(n) \equiv G_N(\varphi_q(n), \varphi_p(n))$ is the discrete Fourier transform defined in the previous section

$$(G_N(n))_{kj} = \frac{1}{\sqrt{N}} e^{-2\pi i(k+\varphi_p(n))(j+\varphi_q(n))/N}. \tag{8}$$

The quantum multibaker operator defined by Eq. (6) will be denoted by $\mathbf{M}$. The evolution of states is given by $|\Psi'\rangle = \mathbf{M}|\Psi\rangle$, and the time dependence of observables Ω in this system is given by

$$\Omega(t) = \mathbf{M}^{\dagger\,t} \Omega \mathbf{M}^t. \tag{9}$$

The two-step construction of the Floquet propagator allows the decomposition of $\mathbf{M}$ into two operators $\mathbf{M} = \mathbf{BT}$. Here $\mathbf{T}$ governs the transport of states to neighboring lattice sites and $\mathbf{B}$ is the block-diagonal operator where each block contains the local quantum baker operator. Thus $\mathbf{T}$ reflects the structure of the lattice and range of particle jumps while $\mathbf{B}$ represents the scattering processes at every site.

To specify the model completely we still have to choose the phases $\varphi_q(n), \varphi_p(n)$. If we make them the same at every lattice site we obtain translationally invariant model which we call *regular* or *uniform* quantum multibaker. If we choose them

---

[b] "Position" and "momentum" representation refer to representations of the internal dynamics on the quantum torus.
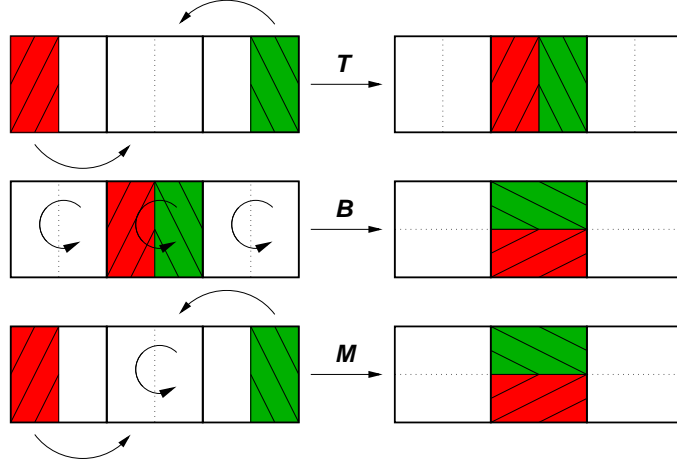
Fig. 2.   Schematic representation of the multibaker model $\mathbf{M}$ as a composition of particle jumps to neighboring cells $\mathbf{T}$ depending on the internal state followed by local randomization of the internal state by the (quantum) baker map $\mathbf{B}$.

randomly from a prescribed, non-trivial distribution we obtain a *disordered* model. Depending on the distribution the obtained models will have different properties, e.g. different localization length, but since this is a one-dimensional system, we expect all of them to exhibit localization. The models which we find particularly attractive for studies are:

(1) Uniform: $\varphi_q(n) = \varphi_q^0, \varphi_p(n) = \varphi_p^0$.
(2) Random: $\varphi_q(n), \varphi_p(n)$ chosen randomly from a uniform distribution on the intervals $[\varphi_q^0, \varphi_q^0 + \varepsilon], [\varphi_p^0, \varphi_p^0 + \delta]$, especially the cases a) $\varepsilon = \delta = 1$, and b) $\delta = 0$ with small ε.
(3) Diluted: $\{\varphi_q(n), \varphi_p(n)\} = \{\varphi_q^0 + \varepsilon, \varphi_p^0 + \delta\}$ with probability p, $\{\varphi_q(n), \varphi_p(n)\} = \{\varphi_q^0, \varphi_p^0\}$ with probability $1 - p$.

Some of their properties will be discussed in later sections of this work.

Currently, no implementation of quantum multibaker maps is available in the literature (apart from $N = 2$ case, see Section 5). We expect that an optical realization of quantum multibaker maps for arbitrary N can be obtained by combining the Bouwmeester et al. [21] implementation of quantum Hadamard walk with the Hannay et al [98] optical implementation of quantum baker map. The implementation of different distributions of phases $\varphi_q(n), \varphi_p(n)$ should also be possible with the ease of shifting phase in optical systems.

3.3. *Quantum multiplexer maps*

To avoid specificity of a single model it is useful to consider more general family of models, where the scatterers are modeled with other local operators than the quantum baker map, interaction range is varied, and lattice has a different structure.

The most general models we are interested in here are those maps on d-dimensional lattices for which the propagator $\mathbf{M}$ can be decomposed into the product of two operators $\mathbf{T}$ and $\mathbf{B}$ such that $\mathbf{T}$ is homogeneous, $\mathbf{B}$ is block-diagonal, and there is a well-defined semi-classical limit of each of the non-zero blocks of $\mathbf{B}$ operator. Such models will be called *quantum multiplexer maps*.

To be more specific consider a d-dimensional lattice span by the lattice vectors $\mathbf{a}_1, \ldots, \mathbf{a}_d$. Let the k neighbors of site $\mathbf{l} = \sum_{i=1}^{d} l_i \mathbf{a}_i \equiv (l_1, \ldots, l_d)$ be defined by lattice vectors $\mathbf{v}_1, \ldots, \mathbf{v}_k$. By this we mean that a particle coming to site $\mathbf{l}$ can be scattered into one of the sites $\mathbf{l} + \mathbf{v}_\varepsilon$. Let the number of scattering channels from $\mathbf{l}$ into $\mathbf{l} + \mathbf{v}_\varepsilon$ be s_ε. Then the Hilbert space of the system H is the simple sum of Hilbert spaces connected with individual sites $H = \oplus_{\mathbf{n}} H(\mathbf{n})$ which are copies of the particle internal Hilbert space. Each space $H(\mathbf{n})$ is the simple sum of s_ε-dimensional spaces $H_\varepsilon(\mathbf{n})$. We will refer to the basis states as $|\mathbf{n}, \varepsilon, i\rangle \in H_\varepsilon(\mathbf{n})$, where $i = 0, 1, \ldots, s_\varepsilon - 1$. If reference to the internal structure is not needed we will write $|\mathbf{n}, i\rangle \in H(\mathbf{n})$, where $i = 0, 1, \ldots, N - 1$, $N = \sum_\varepsilon s_\varepsilon$. We have $|\mathbf{n}, j\rangle \equiv |\mathbf{n}, \varepsilon, i\rangle$ if $j = \sum_{\alpha=1}^{\varepsilon-1} s_\alpha + i$. Then the operator $\mathbf{T}$ in basis $|\mathbf{n}, \varepsilon, i\rangle$ is given by

$$\mathbf{T}_{(\mathbf{m}, \tilde{\varepsilon}, j), (\mathbf{n}, \varepsilon, i)} \equiv \langle \mathbf{m}, \tilde{\varepsilon}, j | \mathbf{T} | \mathbf{n}, \varepsilon, i \rangle = \delta_{\tilde{\varepsilon}, \varepsilon} \delta_{i, j} \delta_{\mathbf{m}, \mathbf{n} + \mathbf{v}_\varepsilon}. \tag{10}$$

Thus the operator $\mathbf{T}$ defines only to which sites the incoming particle can be scattered.
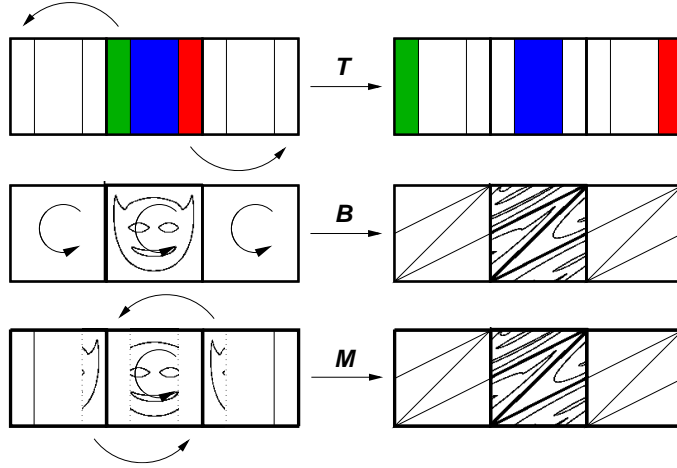

Fig. 3.   Schematic representation of an example multibaker model $\mathbf{M}$. A particle jumps to one of its two nearest neighbors or remains at site depending on its internal state. After a jump the internal state is changed by local action of some operator, in this case (quantum) cat map. Particle jumps to neighboring cells are induced by operator $\mathbf{T}$, local randomization of the internal state is induced by operator $\mathbf{B}$.

The scattering process itself is described by operator $\mathbf{B}$ which is block diagonal $\mathbf{B}_{(\mathbf{m}, j), (\mathbf{n}, i)} \equiv \langle \mathbf{m}, j | \mathbf{B} | \mathbf{n}, i \rangle = \delta_{\mathbf{m}, \mathbf{n}} B(\mathbf{n})_{i, j}$. Local scattering operators $B(\mathbf{n})$ are arbitrary unitary operators of dimension N. In the previous section they were quantum

baker maps. We will usually be interested in diffusive processes so we need a way to randomize dynamics. Thus we will often assume that $B(\mathbf{n})$ is a quantum map with well-defined classical limit, e.g. perturbed cat map, kicked top, or other, which will often be classically chaotic, but can also be mixed, or regular (integrable).

To study how the internal instability (chaos) reflects on the transport properties of the extended system we need to consider a family of such maps parametrized by the dimension of the scattering operator N. To obtain this family we take the same lattice structure and neighbors but we assume the number of scattering channels into neighbor $\mathbf{v}_i$ is $\tilde{s}_i = ms_i$. Thus the dimension of the internal Hilbert space is $\tilde{N} = \sum_i \tilde{s}_i = mN$ and the non-zero blocks of $\tilde{\mathbf{B}}$ are given by the quantum map $B(\mathbf{n})$ in the dimension $\tilde{N}$.

Let us consider some examples to clarify the notations.

(1) Original quantum multibaker described in the previous section. This is a one-dimensional model, there are just two neighbors defined by vectors $v_1 = +1$ and $v_2 = -1$. There are $N/2$ scattering channels outgoing to each of the neighbors, thus the only non-zero elements of $\mathbf{T}$ are $\mathbf{T}_{(l+\varepsilon,\varepsilon,i),(l,\varepsilon,i)}$ for $i = 0, 1, \ldots, N/2-1$, $\varepsilon = \pm 1$. Local scattering operators $B(n)$ are the quantum baker maps, eq. (7).

(2) Consider a square lattice with transport to four nearest neighbors and a non-zero probability of remaining at site. The lattice is spanned by vectors $\mathbf{a}_1 = (1,0)$ and $\mathbf{a}_2 = (0,1)$, the neighbors are defined by vectors $\mathbf{v}_{1,2} = \pm\mathbf{a}_1, \mathbf{v}_{3,4} = \pm\mathbf{a}_2, \mathbf{v}_5 = (0,0)$. Assume $s_\varepsilon = N/6$ for $\varepsilon = 1, 2, 3, 4$, $s_5 = N/3$, and take $N = 6s_0$. Then the only non-zero elements of $\mathbf{T}$ are of the form $\mathbf{T}_{(\mathbf{l}+\mathbf{v}_\varepsilon,\varepsilon,i),(\mathbf{l},\varepsilon,i)}$ for $\varepsilon = 1, 2, 3, 4$ and $i = 0, 1, \ldots, s_0 - 1$ or $\mathbf{T}_{(\mathbf{l},5,i),(\mathbf{l},5,i)}$ for $i = 0, 1, \ldots, 2s_0 - 1$. Local scattering operators are N-dimensional quantum maps, one can take for instance regular quantum baker maps or triadic quantum baker maps.

(3) For a hexagonal lattice spanned by $\mathbf{a}_1 = (1/2, \sqrt{3}/2), \mathbf{a}_2 = (1,0)$ with 12 neighbors we may take $s_i = 2s_0$ for the six nearest neighbors $\pm\mathbf{a}_1, \pm\mathbf{a}_2, \pm(\mathbf{a}_1 - \mathbf{a}_2)$. For second-order neighbors $\pm(\mathbf{a}_1 + \mathbf{a}_2), \pm(2\mathbf{a}_1 - \mathbf{a}_2), \pm(2\mathbf{a}_2 - \mathbf{a}_1)$ we may take $s_i = s_0$. Thus the internal Hilbert space is of dimension $N = 18s_0$.

For every choice of lattice structure we can consider many different scattering operators. We may choose the same operator for every site, e.g. a quantum baker map with fixed phases. We may also choose a family of operators differing from site to site but converging to the same classical map, as in the random quantum multibaker, where every local scattering operator is a quantum baker map with different phases which however all converge to the same classical baker map. One may consider other distributions of the local operators, for instance placement of quantum baker map with fixed phases at a site with probability p and identity operator with probability $1 - p$. This leads to a model of diluted scatterers since identity operator in place of a local scatterer plays the role of empty space: it propagates incoming particles further which follows from the translationally invariant structure of $\mathbf{T}$ operator (Section 4.4.3).

The types of scatterers worth considering depend on the problem of study. We

are mostly interested in the influence of the local instability on the global transport properties. A natural choice for local scatterers are quantum baker maps, since the classical multibaker maps and the quantum baker maps are very well studied. It is also easily tractable, moreover, the classical baker map is equivalent to a coin toss which makes classical multibaker map immediately and apparently a deterministic version of simple random walk. Thus the quantum multibaker map becomes a natural candidate for a model of quantum random walk. One may also consider other variants of quantum baker maps, which share the advantages and disadvantages of the original, but may be adapted to the structure of transfer matrix $\mathbf{T}$. For instance one can use a triadic map in dimension $N = 3s_0$

$$G_N^{-1}(n) \cdot \begin{bmatrix} G_{N/3}(n) & 0 & 0 \\ 0 & G_{N/3}(n) & 0 \\ 0 & 0 & G_{N/3}(n) \end{bmatrix}$$

or for $N = 4s_0$

$$G_N^{-1}(n) \cdot \begin{bmatrix} G_{N/4}(n) & 0 & 0 \\ 0 & G_{N/2}(n) & 0 \\ 0 & 0 & G_{N/4}(n) \end{bmatrix}$$

with the two outer stripes connected with transfer to the two nearest neighbors in 1D case, and the middle stripe with the states remaining at site. The last case leads to classical probability of remaining at site $1/2$ and probabilities of $1/4$ of jumping to one of the two neighbors.

The disadvantages of the baker map as a paradigm for the study of quantum chaos are its discontinuity and the impossibility of introducing regular islands in the phase space. Thus in the quantum multibakers one cannot study the changes in transport when the character of local dynamics changes from regular, through mixed, to chaotic. To avoid these problems one may consider locally dynamics of other maps, such as perturbed cat maps [19,43] or quantum kicked top [95,96].

When completely random scatterers are needed it may be useful to take as local operators completely random matrices from CUE or COE ensembles. This approach is viable both numerically and analytically.

4. Properties of quantum multiplexer models

4.1. *Regular and random case with periodic boundary conditions*

The structure of eigenstates and of spectrum depends crucially on the distribution of local scattering operators $B(n)$. For regular quantum multiplexer maps, where the scattering operator is the same at every site, the eigenstates are extended and the spectrum is banded. Thus on d-dimensional lattice of length L in every direction an eigenstate Ψ is of the form $\Psi_\varepsilon(n) = \exp(i\kappa \cdot \mathbf{n})\tilde{\Psi}_\varepsilon$. Here $\tilde{\Psi}_\varepsilon$ is an eigenvector of N-dimensional modified operator $\tilde{B}_\kappa$ defined by

$$\tilde{B}_{\kappa;\varepsilon_2,\varepsilon_1} := B_{\varepsilon_2,\varepsilon_1} e^{-i\kappa \cdot \mathbf{v}_{\varepsilon_1}} \tag{11}$$

where κ has the form $\frac{2\pi}{L}(k_1, k_2, \ldots, k_d)$. The spectrum of the whole system consists of the spectra of all the $\tilde{B}$ operators.

In a specific example of a regular dyadic quantum multibaker map on one-dimensional lattice with periodic boundary conditions[208] every eigenstate has a Bloch form

$$\Psi_\pm(n) = \exp(i\kappa n)\tilde{\Psi}_\pm/\sqrt{L}, \tag{12}$$

where $\begin{bmatrix} \tilde{\Psi}_+ \\ \tilde{\Psi}_- \end{bmatrix}$ is the normalized eigenstate of a modified quantum baker operator

$$G_N^{-1}\begin{bmatrix} G_{N/2}e^{-i\kappa} & 0 \\ 0 & G_{N/2}e^{i\kappa} \end{bmatrix}. \tag{13}$$

Periodic boundary conditions imply $e^{i\kappa L} = 1$, which leads to $\kappa_k = 2\pi k/L, k = 0, 1, \ldots, L - 1$. For every κ_k there are N eigenstates, which gives together NL eigenstates. For $N = 2$ internal states[208] the eigenvalues are given by

$$\lambda_{\pm,k} = \frac{e^{i\beta}}{\sqrt{2}}\left[\cos(\alpha + 2k\pi/L) \pm i\sqrt{1 + \sin^2(\alpha + 2k\pi/L)}\right], \tag{14}$$

with

$$\alpha = (1 + \varphi_q + \varphi_p)\pi/2, \qquad \beta = (1 + \varphi_q + \varphi_p - 2\varphi_q\varphi_p)\pi/2 = \alpha - \pi\varphi_q\varphi_p. \tag{15}$$

Clearly, $\lambda = e^{i\omega}$ lie on the unit circle and the "quasi-energies" ω lie in two bands of length $\pi/2$ symmetric with respect to the center of the unit circle. The exact location depends upon the phases φ_q, φ_p and is given by $\omega - \beta \in [\pi/4, 3\pi/4] \cup [5\pi/4, 7\pi/4]$. When α is an integer multiple of π/L the spectrum is doubly degenerate. This non-generic case happens for instance for the most common choices of phases ($\varphi_q = \varphi_p = 1/2$ for every lattice, or $\varphi_q = \varphi_p = 0$ for even lattices).
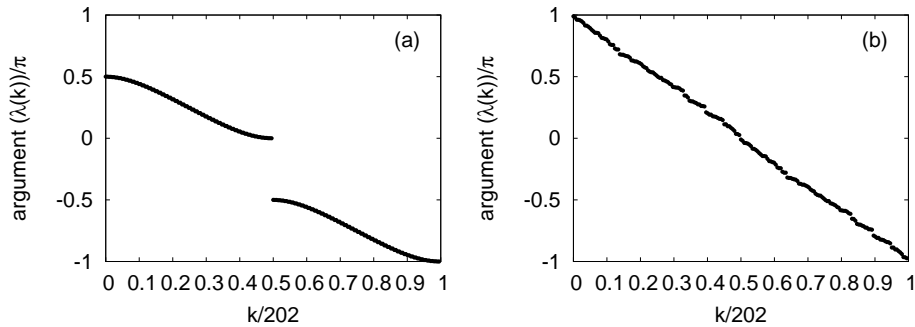

Fig. 4. Eigenspectra of closed quantum multibaker maps for chains of length $L = 101$ cells with periodic boundary conditions. (a) Periodic case with phases $\varphi_q = \varphi_p = 1/2, \alpha = \pi, \beta = 3\pi/4$. (b) One realization of the random case with $\varphi_q(n) = \varphi_p(n) \in [0, 1[$.

To analyze the spectrum and the structure of eigenstates of open systems and of the disordered case it is convenient to rephrase the eigenvalue problem in terms

of transfer matrices[12,150,182,208]. We will restrict ourselves to the dyadic quantum multiplexer map to balance between generality and clarity.

Dyadic quantum multiplexer is defined locally by

$$\begin{bmatrix} \Psi^+(n,t+1) \\ \Psi^-(n,t+1) \end{bmatrix} = B(n) \begin{bmatrix} \Psi^+(n-1,t) \\ \Psi^-(n+1,t) \end{bmatrix}, \tag{16}$$

where the local scattering operators $B(n)$ can be decomposed as

$$B(n) = \begin{bmatrix} B^+_+(n) & B^+_-(n) \\ B^-_+(n) & B^-_-(n) \end{bmatrix}.$$

Symbol $B^\alpha_\beta(n)$ denotes the $N/2 \times N/2$ block of the operator $\mathbf{B}$ in the basis $|n,\alpha,i\rangle$ consisting of elements $\mathbf{B}_{(n,\alpha,i),(n,\beta,j)} \equiv \langle n,\alpha,i|\mathbf{B}|n,\beta,j\rangle$. Similarly $\Psi^\alpha(n)$ is the $N/2$ vector consisting of elements $\langle n,\alpha,i|\Psi\rangle$. The notation is motivated by the fact that $\Psi^\alpha(n)$ is transferred in one time step into $\Psi^\pm(n+\alpha)$. We write $\pm$ for ± 1. Thus the eigenvalue equation for the system can be written as

$$\lambda \begin{bmatrix} \Psi^+(n) \\ \Psi^-(n) \end{bmatrix} = \begin{bmatrix} B^+_+(n) & B^+_-(n) \\ B^-_+(n) & B^-_-(n) \end{bmatrix} \begin{bmatrix} \Psi^+(n-1) \\ \Psi^-(n+1) \end{bmatrix}. \tag{17}$$

We can rewrite this equation in terms of transfer matrix $T_\lambda(n)$ so that

$$\begin{bmatrix} \Psi^+(n) \\ \Psi^-(n+1) \end{bmatrix} = T_\lambda(n) \cdot \begin{bmatrix} \Psi^+(n-1) \\ \Psi^-(n) \end{bmatrix} \tag{18}$$

with

$$T_\lambda(n) = \begin{bmatrix} \{B^+_+(n) - B^+_-(n)[B^-_-(n)]^{-1}B^-_+(n)\}/\lambda & B^+_-(n)[B^-_-(n)]^{-1} \\ -[B^-_-(n)]^{-1}B^-_+(n) & \lambda[B^-_-(n)]^{-1} \end{bmatrix}. \tag{19}$$

With the help of transfer matrices we can rewrite the equation for eigenvalues for general dyadic quantum multiplexer map with periodic boundary conditions (but not necessarily regular) as

$$\det(\mathbb{I} - \prod_{n=0}^{L-1} T_\lambda(n)) = 0, \tag{20}$$

where $\mathbb{I}$ is the $N \times N$ identity matrix.

For a regular system where $T_\lambda(n) \equiv T_\lambda$ this is equivalent to the statement that one of the eigenvalues of T_λ is L-th root of 1. In the special case of $N = 2$ quantum multibaker[208]

$$B(n) = \frac{1}{\sqrt{2}} \begin{bmatrix} e^{-i\pi\varphi_q\varphi_p} & e^{i\pi\varphi_q(1-\varphi_p)} \\ e^{i\pi\varphi_p(1-\varphi_q)} & e^{i\pi(1+\varphi_q+\varphi_p-\varphi_q\varphi_p)} \end{bmatrix} \tag{21}$$

the transfer matrix takes form

$$T_\lambda(n) = \begin{bmatrix} \sqrt{2}e^{-i\pi\varphi_q\varphi_p}/\lambda & -e^{-i\pi\varphi_p} \\ e^{-i\pi\varphi_q} & \sqrt{2}\lambda e^{-i\pi(1+\varphi_q+\varphi_p-\varphi_q\varphi_p)} \end{bmatrix}. \tag{22}$$

The eigenvalues χ of T satisfy equation

$$\chi e^{i\alpha} + \frac{1}{\chi e^{i\alpha}} = \sqrt{2}\left(\frac{\lambda}{e^{i\beta}} + \frac{e^{i\beta}}{\lambda}\right). \tag{23}$$

Then, the condition (20) implies $\chi^L = 1$. Solving (23) for λ we obtain (14) again. The structure of eigenstates reflects the periodicity of the lattice: $\begin{bmatrix} \Psi_+(0) \\ \Psi_-(1) \end{bmatrix}$ for k-th eigenstate is the eigenvector of T_λ corresponding to $\chi_k = \exp(i2\pi k/L)$, and $\Psi_\pm(n) = \chi_k^n \Psi_\pm(0)$.

In random system, where the phases φ_q, φ_p defining the map are chosen randomly from a uniform distribution on unit interval at each cell, one has to consider the distribution of all the possible products. The numerically obtained quasi-energy spectrum for one example realization is illustrated in Figure 4 (b) and can be compared with that for the uniform case. In this case it is of interest to rewrite the eigenequations in yet another form to separate the Ψ^+ from Ψ^- states. The result is similar in form to the Anderson model[7,208]. For Ψ^+ we obtain

$$\begin{bmatrix} \Psi^+(n) \\ \Psi^+(n-1) \end{bmatrix} = \begin{bmatrix} K(n,n-1) & L(n,n-1) \\ \mathbb{I} & \mathbb{O} \end{bmatrix} \cdot \begin{bmatrix} \Psi^+(n-1) \\ \Psi^+(n-2) \end{bmatrix}, \tag{24}$$

where

$$K(n,n-1) = \lambda^{-1}B^+_+(n) - \lambda^{-1}B^+_-(n)[B^-_-(n)]^{-1}B^-_+(n)$$
$$+ \lambda B^+_-(n)[B^-_-(n)]^{-1}[B^+_-(n-1)]^{-1},$$
$$L(n,n-1) = -B^+_-(n)[B^-_-(n)]^{-1}[B^+_-(n-1)]^{-1}B^+_+(n-1).$$

In the case $N = 2$ we can evaluate these expressions as

$$K = \sqrt{2}e^{-i\alpha}\left[\frac{1}{\lambda}e^{i\beta} + \lambda e^{-i\gamma}e^{-i(\tilde{\beta}-\tilde{\gamma})}\right]$$
$$L = -e^{-i(\gamma+\alpha)}e^{i(\tilde{\gamma}-\tilde{\alpha})}$$

where $\gamma = (\varphi_p - \varphi_q)\pi/2$, and the variables with tilde are defined in terms of the phases from cell $n-1$, $\varphi_q(n-1), \varphi_p(n-1)$. We rewrite this equation so that it takes the form a dynamical problem, where the cell index n plays the role of the time step

$$\Psi^+(n) = 2\sqrt{2}e^{i\varphi_1}\cos(\varphi_3)\Psi^+(n-1) - e^{i\varphi_2}\Psi^+(n-2),$$

or, using transfer matrices,

$$\begin{bmatrix} \Psi^+(n) \\ \Psi^+(n-1) \end{bmatrix} = \begin{bmatrix} 2\sqrt{2}e^{i\varphi_1}\cos(\varphi_3) & -e^{i\varphi_2} \\ 1 & 0 \end{bmatrix}\begin{bmatrix} \Psi^+(n-1) \\ \Psi^+(n-2) \end{bmatrix}. \tag{25}$$

The phases are given by

$$\varphi_1 = -\alpha + (\beta - \gamma)/2 - (\tilde{\beta} - \tilde{\gamma})/2,$$
$$\varphi_2 = -(\gamma + \alpha) + (\tilde{\gamma} - \tilde{\alpha}),$$
$$\varphi_3 = \omega - (\beta + \gamma)/2 - (\tilde{\beta} - \tilde{\gamma})/2.$$

16   *Daniel K. Wójcik*

The transfer matrix can also be written as

$$\begin{bmatrix} e^{i\varphi_1} & 0 \\ 0 & 1 \end{bmatrix} \begin{bmatrix} 2\sqrt{2}\cos(\varphi_3) & -1 \\ 1 & 0 \end{bmatrix} \begin{bmatrix} 1 & 0 \\ 0 & e^{i\varphi_2} \end{bmatrix} \tag{26}$$

to make the similarity with Anderson model more apparent.

As expected, the eigenstates are localized with localization becoming more pronounced with increasing length L of the system. Figure 5 shows three sample eigenstates of a realization of the quantum random multibaker of length $L = 101$ with periodic boundary conditions on logarithmic (a) and regular (b) scale. Absolute values of $\Psi^+(n)$ are shown. Absolute values of $\Psi^-(n)$ are not shown because they
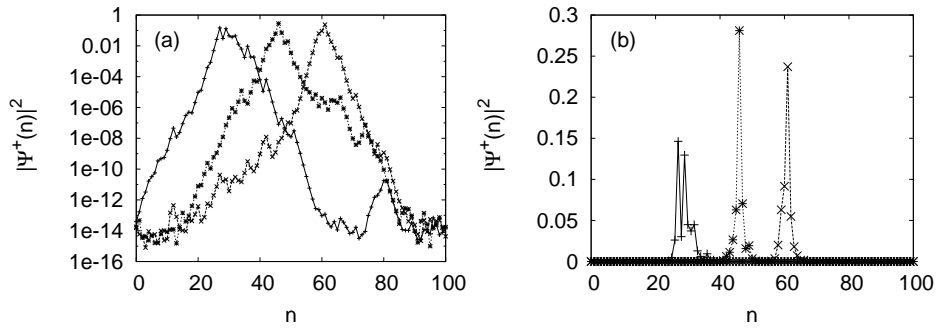

Fig. 5.   Three examples out of 202 eigenstates of a realization of the quantum random multibaker of length $L = 101$ and $N = 2$ with periodic boundary conditions on logarithmic (a) and regular (b) scale. Absolute values of $\Psi^+(n)$ are shown.

are almost identical (the difference is on the order of less than 10^{-6}). To understand this phenomenon let us investigate the currents associated with the eigenstates.

From the evolution equation (16) and unitarity of $B(n)$ we can calculate the change in the probability density at a given lattice site due to the flow between the site and its neighbors

$$\varrho(n, t+1) - \varrho(n, t) = J_{n-1|n} - J_{n|n+1}, \tag{27}$$

where $\varrho(n, t) = \varrho_+(n, t) + \varrho_-(n, t)$, $\varrho_\varepsilon(n, t) = \Psi^\varepsilon(n, t)^\dagger \Psi^\varepsilon(n, t)$, for $\varepsilon = \pm$, and the current

$$J_{n-1|n}(t) = \varrho_+(n-1, t) - \varrho_-(n, t) \tag{28}$$

is the difference between the probability incoming from site $n-1$ to site n and the probability outgoing from n to $n-1$.

For stationary solutions such as eigenstates and steady states discussed later on the current is independent of time. Moreover, since $T_n^\dagger \begin{bmatrix} -1 & 0 \\ 0 & 1 \end{bmatrix} T_n = \begin{bmatrix} -1 & 0 \\ 0 & 1 \end{bmatrix}$, the current between every two neighbors is the same for a given eigenstate. The distribution of the current values for different eigenstates for systems of length

$L = 128, 256, 512, 1024$ superimposed for regular and random QMBs with $N = 2$ is shown at Figure 6(a). We observe that the distribution of currents is scaling
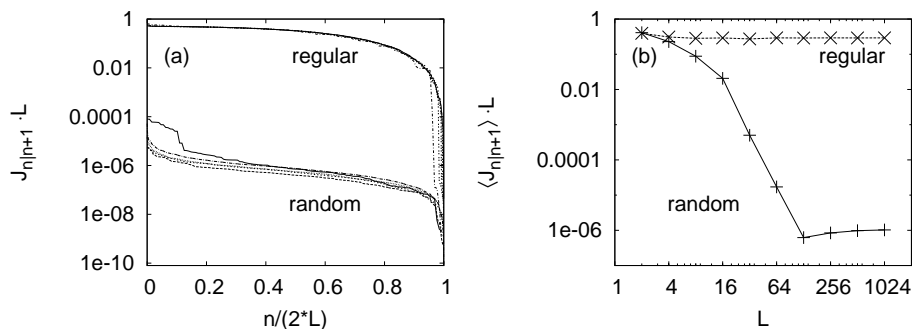

Fig. 6.   (a) Distribution of the current values for different eigenstates for systems of length $L = 128, 256, 512, 1024$ superimposed for regular and random QMBs with $N = 2$. (b) The mean current for the same systems where the average has been taken over all the states for the given system.

inversely with the system size L, in both random and regular case. However, the difference in values between the two cases is six orders of magnitude. To take this into account each distribution in Figure 6 (a) is multiplied by system length and rescaled to fit in the interval $[0, 1]$. Figure 6 (b) shows the mean current with average taken over all the states. It shows how the system properties dramatically change with the increase of its size.

4.2. *Regular case with absorbing boundary conditions: escape rate*

To study the properties of quantum multiplexer maps with absorbing boundary conditions we find it most convenient to use the formulation of dynamics in terms of transfer matrices (18). Here we consider dyadic quantum multiplexer maps with open boundaries. In the classical case, open boundaries are important for the application of the escape-rate formalism of Gaspard and Nicolis[83] which relates the rate of decay of the initial number of particles on a large, open chain to the diffusion coefficient, and then to the Lyapunov exponents and the Kolmogorov-Sinai entropy of trajectories on a fractal repeller, *i.e.* the set of initial points for trajectories that never leave the chain[46,74].

Let us consider dyadic quantum multiplexer defined locally by eq. (16) in the cells $n = 1, 2, \ldots, L - 2$. At the boundary the states which would be transmitted out of the chain are absorbed, that is we require

$$\begin{bmatrix} \Psi^+(0, t+1) \\ \Psi^-(0, t+1) \end{bmatrix} = B(0) \begin{bmatrix} \mathbb{O}_{\frac{N}{2} \times 1} \\ \Psi^-(1, t) \end{bmatrix}, \tag{29}$$

and

$$\begin{bmatrix} \Psi^+(L-1,t+1) \\ \Psi^-(L-1,t+1) \end{bmatrix} = B(L-1) \begin{bmatrix} \Psi^+(L-2,t) \\ \mathbb{O}_{\frac{N}{2}\times 1} \end{bmatrix}. \tag{30}$$

This way the probability to remain in the system decays since nothing enters the system from the outside and $|\Psi^-(0,t)|^2 + |\Psi^+(L-1,t)|^2$ are absorbed. Due to the escape of probability density, the eigenvalues which determine the time dependence of the probability density in each cell move to the interior of the unit circle.

If λ is an eigenvalue of the system and Ψ the corresponding eigenstate then (18) is satisfied with $T_\lambda(n)$ given by (19). Taking into account the boundary conditions (29) and (30) we obtain

$$\begin{bmatrix} \Psi^+(L-1) \\ 0_{\frac{N}{2}\times 1} \end{bmatrix} = T_\lambda(L-1) \cdot \ldots \cdot T_\lambda(1) \cdot T_\lambda(0) \cdot \begin{bmatrix} 0_{\frac{N}{2}\times 1} \\ \Psi^-(0) \end{bmatrix}. \tag{31}$$

Therefore, the condition defining the spectrum and the eigenstates can be phrased as follows: λ is an eigenvalue if $\det V = 0$, where

$$V = [\mathbb{O}_{\frac{N}{2}\times\frac{N}{2}}\ \mathbb{I}_{\frac{N}{2}\times\frac{N}{2}}] \cdot T_\lambda(L-1) \cdot \ldots \cdot T_\lambda(1) \cdot T_\lambda(0) \cdot \begin{bmatrix} \mathbb{O}_{\frac{N}{2}\times\frac{N}{2}} \\ \mathbb{I}_{\frac{N}{2}\times\frac{N}{2}} \end{bmatrix}, \tag{32}$$

and $\Psi^-(0)$ is the eigenstate of V belonging to its kernel.

In case of regular dyadic quantum multibaker map in the deep quantum regime, i.e. for $B(n) \equiv B$ a quantum baker map with fixed phases and for $N = 2$, one can get more analytical insight[208]. In this case B and T are given by the equations (21) and (22). The eigenvalues $\chi_\pm$ of T and λ of the whole system satisfy eq. (23). If we set $u = \chi e^{i\alpha}$, $v = \lambda/e^{i\beta}$ we obtain the relation between u and v

$$v + \frac{1}{v} = \frac{1}{\sqrt{2}}\left[u + \frac{1}{u}\right], \tag{33}$$

The two solutions u_+, u_- satisfy $u_+ u_- = 1$, and $u_+ + u_- = \sqrt{2}[v + 1/v]$. Since $|v| = |\lambda| < 1$, it follows that u_+, u_- do not lie on the unit circle. In particular, they must be different and so the matrix T is non-degenerate. We take $|u_+| > 1 > |u_-|$ to define them uniquely, and use $u_\pm = \chi_\pm e^{i\alpha}$. If we set $u_\pm = e^{\pm i\kappa}$, and then solve for v we obtain

$$v_\pm = \frac{1}{\sqrt{2}}[\cos\kappa \pm i\sqrt{1 + \sin^2\kappa}]. \tag{34}$$

Interesting solutions are those where κ is not purely real, that is, $\kappa \in \mathbb{C} \setminus \mathbb{R}$. Then the product T^L is given by

$$\begin{aligned} T^L &= \frac{\chi_+^L - \chi_-^L}{\chi_+ - \chi_-}T - \frac{\chi_-\chi_+^L - \chi_+\chi_-^L}{\chi_+ - \chi_-}I \\ &= \frac{e^{-i\alpha L}}{\sin\kappa}\left\{\sin L\kappa\, T\, e^{i\alpha} - \sin(L-1)\kappa\,\mathbb{I}\right\} \\ &= \frac{e^{-i\alpha L}}{\sin\kappa}\left\{\sin(L\kappa)\begin{bmatrix} \sqrt{2}/v & -e^{i(\alpha-\pi\varphi_p)} \\ e^{i(\alpha-\pi\varphi_q)} & \sqrt{2}v \end{bmatrix} - \sin((L-1)\kappa)\begin{bmatrix} 1 & 0 \\ 0 & 1 \end{bmatrix}\right\} \end{aligned} \tag{35}$$

Therefore $\det V = 0$ implies

$$\sqrt{2}v \sin L\kappa - \sin(L-1)\kappa = 0.$$

With the help of (33) we obtain a very simple equation

$$\sin^2 L\kappa + \sin^2 \kappa = 0. \tag{36}$$

The only real solutions of this equation are $\kappa = k\pi$, $k \in \mathbb{Z}$, but, as mentioned above, they must be discarded. If we write Eq. (36) as

$$\sin L\kappa = i\delta \sin \kappa, \tag{37}$$

where $\delta = \pm 1$, we can solve it perturbatively expanding κ in powers of δ about $\kappa = k\pi/L$, $k = 1, \ldots, L-1$ at the end setting $\delta = \pm 1$. This approach gives results which quickly converge numerically, for all allowed values of k. In the second order of approximation we obtain[208]

$$\lambda = \frac{e^{i\beta}}{\sqrt{2}} \left(a + i\delta \sqrt{1+b^2} \right) \exp\left\{ -\frac{b^2}{L\sqrt{1+b^2}} \right\} \exp\left\{ -\frac{i\delta ab^2 \left(2\,b^2 + 3\right)}{2L^2 \left(1+b^2\right)^{3/2}} \right\}, \tag{38}$$

where $a = \cos(k\pi/L)$ and $b = \sin(k\pi/L)$. The non-exponential factor on the right hand side is the unperturbed solution. Figure 4.2 shows the absolute value of v (in the fourth order approximation).
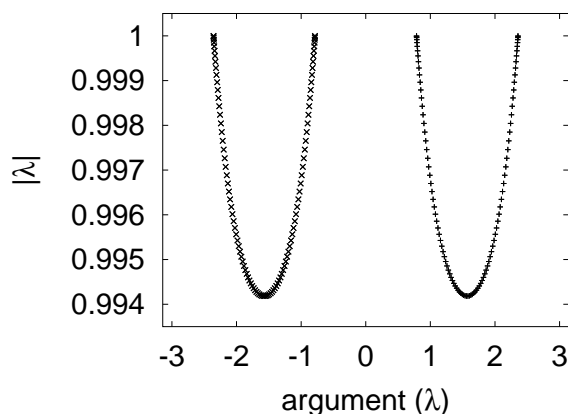

Fig. 7.   Amplitude versus argument of the eigenvalues of an open quantum multibaker chain of length $L = 101$, $N = 2$ in the fourth order of approximation.

Another estimate of the eigenvalues nearest to the unit circle ($k \in \{1, L-1, L+1, 2L-1\}$) in the large-size limit can be obtained through an expansion of Eq. (37) in powers of L^{-1}. While this leads to an asymptotic solution for v which quickly diverges for most k, it gives us a faster converging approximation for the leading

order behavior of $k \ll L$

$$v(k) \approx \exp\left[\pm i\left(\frac{\pi}{4} + \frac{k^2\pi^2}{2L^2}\right)\right] \exp\frac{-k^2\pi^2}{L^3}. \tag{39}$$

The escape of probability density from an open system asymptotically is dominated by the eigenvalue closest to the unit circle. Therefore the escape rate

$$\gamma := -\lim_{t\to\infty}\frac{\log P(t)}{t} \tag{40}$$

of the regular quantum multibaker map is given by

$$\gamma = -\log|v(1)|^2 \approx \frac{2\pi^2}{L^3}. \tag{41}$$

Thus even though the motion *inside* the quantum multibaker is *faster* (ballistic) than in the corresponding classical system (diffusive), the *effusion* (decay of probability density) is *slower* than that for the corresponding classical system[74]

$$\gamma_{\text{class}} = \frac{\pi^2}{2L^2}. \tag{42}$$

In their study of quantum scattering resonances for an open, periodic chain of scatterers, in high energy limit Barra and Gaspard[12] found that the logarithms of the magnitudes of the eigenvalues can be bounded above and below by functions that scale as $1/L$. They expect that the lower bound, given by the eigenvalues in the middle of the band, should hold also for lower energies[c]. On the other hand, the upper bound, which gives the escape rate, is given by the resonances near the edges of the bands which are harder to estimate at low energies. Therefore this bound is more difficult to control.

This reasoning is consistent with our findings. In our case, the eigenvalues of the smallest magnitude are those for which to $k \approx \pm L/2$ (the middle of the band; see Figure 4.2). Thus their magnitude can be estimated from (38) setting $a = 0, b = 1$ and therefore their logarithms scale as $1/L$. On the other hand, the eigenvalues of largest magnitude, which give the escape rate, lie at the edges of the band.

The discrepancy between our results is not surprising because the high-energy limit corresponds to semi-classical limit for our system, while here we consider the extreme quantum case.

4.3. *Regular case with flux boundary conditions: steady states, continuity equation, and the current*

Let us now consider transmission through a dyadic quantum multiplexer. We take the system of length L and couple it at both ends to infinitely conducting leads[69,187,208]. We model the leads by a local operator proportional to identity and assume traveling waves in the leads moving to the right and to the left. Thus to the

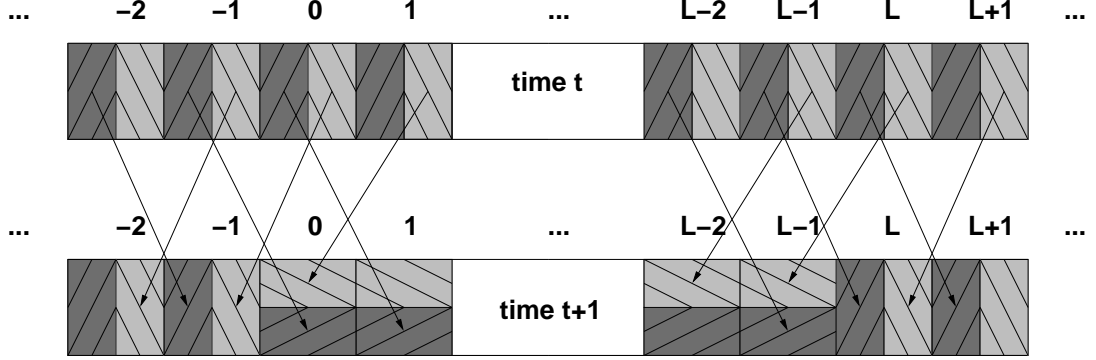----

[c]P. Gaspard, private communication

Fig. 8.   Scattering from a quantum multibaker. Local scattering operators $B(n)$ in cells 0 to $L-1$ are given by quantum baker maps. Local dynamics in the leads is trivial, $B(n) \propto \mathbb{I}$.

left of the chain, $n < 0$, we have a traveling wave

$$\Psi^+(n,t) = Ae^{i(\omega t - kn)}, \tag{43}$$

$$\Psi^-(n,t) = Be^{i(\omega t + kn)}, \tag{44}$$

and to the right of the chain, $n > L - 1$, the wave is given by

$$\Psi^+(n,t) = Ce^{i(\omega t - kn)}, \tag{45}$$

$$\Psi^-(n,t) = De^{i(\omega t + kn)}. \tag{46}$$

Here A, D, are the amplitudes of the incoming waves, while B, C, are the amplitudes of the outgoing waves. Such solutions are consistent with the quantum multiplexer framework as described in Section 3.3 with local operators $B(n)$ given by $e^{i(\omega - k)}I$ for $n > L - 1$ and $n < 0$.

The dynamics inside the system is again given by eq. (16) with the boundary conditions induced by the incoming currents:

$$\Psi^+(-1,t) = Ae^{i(\omega t + k)}, \tag{47}$$

$$\Psi^-(L,t) = De^{i(\omega t + Lk)}. \tag{48}$$

We will use a scattering approach to find the outgoing amplitudes, B, C, for the steady state solution, as well as to solve the problem of the relaxation of some initial state to a steady state. First we consider the steady state solution for the quantum multibaker chain with conducting leads.

The steady state solution is defined by the condition that the time dependence of the wave function can be incorporated in a time dependent phase factor. This is consistent with the boundary conditions only when $\Psi^\pm(n, t+1) = e^{i\omega}\Psi^\pm(n,t)$ which implies $\Psi^\pm(n,t) = e^{i\omega t}\Psi^\pm(n)$, where we write $\Psi^\pm(n) \equiv \Psi^\pm(n, 0)$. Therefore, the steady state equation has the same form as the eigenvalue equation for a closed system (17) with $e^{i\omega}$ replacing λ:

$$e^{i\omega} \begin{bmatrix} \Psi^+(n) \\ \Psi^-(n) \end{bmatrix} = \begin{bmatrix} B^+_+(n) \; B^+_-(n) \\ B^-_+(n) \; B^-_-(n) \end{bmatrix} \begin{bmatrix} \Psi^+(n-1) \\ \Psi^-(n+1) \end{bmatrix}. \tag{49}$$

22   *Daniel K. Wójcik*

The transmission and reflection coefficients for the chain can be expressed in terms of the scattering S-matrix, given by

$$\begin{bmatrix} \Psi^-(0) \\ \Psi^+(L-1) \end{bmatrix} = S_{0,L-1} \begin{bmatrix} \Psi^+(-1) \\ \Psi^-(L) \end{bmatrix}, \tag{50}$$

where the elements of S-matrix are

$$S_{0,L-1} = \begin{bmatrix} r_{0,L-1} & t'_{0,L-1} \\ t_{0,L-1} & r'_{0,L-1} \end{bmatrix}. \tag{51}$$

Here the unprimed coefficients refer to waves incident on the left end of the chain, while the primed quantities refer to the waves incident on the right side of the chain. The transmission and reflection coefficients, T, T', R, R' respectively, are then obtained from the elements of S by

$$T = |t_{0,L-1}|^2, \qquad R = |r_{0,L-1}|^2, \tag{52}$$

and similarly for the primed quantities. Unitarity of S implies $T = T'$, $R = R'$. In order to calculate the S-matrix, $S_{0,L-1}$, for the chain, we proceed as for the absorbing case, by looking at the transfer and scattering matrices for one cell, and building up the matrices for the chain by iteration, cell by cell. Consider the cell labelled by the index n. The S-matrix for the n-th cell is given by

$$\begin{bmatrix} \Psi^-(n) \\ \Psi^+(n) \end{bmatrix} = S_n \begin{bmatrix} \Psi^+(n-1) \\ \Psi^-(n+1) \end{bmatrix}, \tag{53}$$

and the transfer T-matrix is

$$\begin{bmatrix} \Psi^+(n) \\ \Psi^-(n+1) \end{bmatrix} = T_n \begin{bmatrix} \Psi^+(n-1) \\ \Psi^-(n) \end{bmatrix}. \tag{54}$$

Each of the matrices can be given in terms of the other, thus,

$$S = \begin{bmatrix} r & t' \\ t & r' \end{bmatrix} \Rightarrow T = \begin{bmatrix} t - r't'^{-1}r & r't'^{-1} \\ -t'^{-1}r & t'^{-1} \end{bmatrix}, \tag{55}$$

$$T = \begin{bmatrix} \alpha & \gamma \\ \beta & \delta \end{bmatrix} \Rightarrow S = \begin{bmatrix} -\delta^{-1}\beta & \delta^{-1} \\ \alpha - \gamma\delta^{-1}\beta & \gamma\delta^{-1} \end{bmatrix}. \tag{56}$$

From the dynamical equations (17) we obtain the S-matrix immediately

$$\begin{bmatrix} \Psi^-(n) \\ \Psi^+(n) \end{bmatrix} = e^{-i\omega} \begin{bmatrix} B^-_+(n) & B^-_-(n) \\ B^+_+(n) & B^+_-(n) \end{bmatrix} \begin{bmatrix} \Psi^+(n-1) \\ \Psi^-(n+1) \end{bmatrix}. \tag{57}$$

which leads to the transfer matrix (19)

$$T(n) = \begin{bmatrix} e^{-i\omega}\{B^+_+(n) - B^+_-(n)[B^-_-(n)]^{-1}B^-_+(n)\} & B^+_-(n)[B^-_-(n)]^{-1} \\ -[B^-_-(n)]^{-1}B^-_+(n) & e^{i\omega}B^-_-(n) \end{bmatrix}. \tag{58}$$

Specializing to the case $N = 2$ these matrices take the form

$$S_n = \frac{e^{-i\omega}}{\sqrt{2}} \begin{bmatrix} e^{i\pi\varphi_p(1-\varphi_q)} & e^{i\pi(1+\varphi_q+\varphi_p-\varphi_q\varphi_p)} \\ e^{-i\pi\varphi_q\varphi_p} & e^{i\pi\varphi_q(1-\varphi_p)} \end{bmatrix} \tag{59}$$

and

$$T_n = \begin{bmatrix} \sqrt{2}e^{-i\omega}e^{-i\pi\varphi_q\varphi_p} & -e^{-i\pi\varphi_p} \\ e^{-i\pi\varphi_q} & \sqrt{2}e^{i\omega}e^{-i\pi(1+\varphi_q+\varphi_p-\varphi_q\varphi_p)} \end{bmatrix}. \tag{60}$$

which is equivalent to (22) if we replace λ with $e^{i\omega}$.

The scattering matrix for the whole multibaker $S_{0,L-1}$ can easily be derived from $T_{0,L-1} := T_{L-1} \cdot \ldots \cdot T_1 \cdot T_0$. Its unitarity can also be verified. For the regular system

$$T_{0,L-1} = T^L = \frac{\chi_+^L - \chi_-^L}{\chi_+ - \chi_-}T - \frac{\chi_-\chi_+^L - \chi_+\chi_-^L}{\chi_+ - \chi_-}I \tag{61}$$

where $\chi_\pm$ are roots of characteristic polynomial of T

$$\chi_\pm = e^{-i\alpha}[\sqrt{2}\cos(\beta - \omega) \pm \sqrt{\cos 2(\beta - \omega)}], \tag{62}$$

and α, β are given by Eq. (15). Depending on the sign of $\cos 2(\beta - \omega)$ there are two types of solutions: if the frequency of the incident wave falls in one of the quasi-energy bands

$$\cos 2(\beta - \omega) < 0 \Leftrightarrow \omega - \beta \in [\pi/4, 3\pi/4] \cup [5\pi/4, 7\pi/4], \tag{63}$$

we have the oscillatory case with some interesting structure. Otherwise, when the frequency of the incident wave falls in the gap, we observe almost total reflection of particles coming from the leads to the chain, becoming total as $L \to \infty$ (the exponential case).

(1) If $\cos 2(\beta - \omega) < 0$ (oscillatory case), the characteristic roots are:

$$\chi_\pm = e^{-i\alpha}[\sqrt{2}\cos(\beta - \omega) \pm i\sqrt{-\cos 2(\beta - \omega)}], \tag{64}$$

thus $|\chi_\pm|^2 = 1$. Set $\chi_\pm = e^{-i\alpha}e^{\pm i\kappa}$. Then the scattering matrix for the chain becomes,

$$S_{0,L-1} = \frac{1}{z_L}\begin{bmatrix} -\sin L\kappa\, e^{i(\alpha - \pi\varphi_q)} & \sin\kappa\, e^{i\alpha L} \\ \sin\kappa\, e^{-i\alpha L} & -\sin L\kappa\, e^{i(\alpha - \pi\varphi_p)} \end{bmatrix}. \tag{65}$$

To simplify the formulas we introduce symbol

$$z_n \equiv r_n e^{i\varphi_n} := \sqrt{2}\sin n\kappa e^{-i(\beta - \omega)} - \sin\kappa(n-1) \tag{66}$$
$$= \cos\kappa n \sin\kappa - i\varepsilon\sin n\kappa\sqrt{1 + \sin^2\kappa},$$

where $\varepsilon = \pm$ is the sign of $\sin(\beta - \omega)$. Some of its properties are given in Appendix A. Then the transmission and reflection coefficients are

$$R = \frac{\sin^2 L\kappa}{\sin^2\kappa + \sin^2 L\kappa} = \frac{1}{1 + \frac{\sin^2\kappa}{\sin^2 L\kappa}}, \tag{67}$$

$$T = \frac{\sin^2\kappa}{\sin^2\kappa + \sin^2 L\kappa} = \frac{1}{1 + \frac{\sin^2 L\kappa}{\sin^2\kappa}}. \tag{68}$$

Some interesting special cases occur when:

(a) $\kappa = m\pi + \pi/2$, L odd: $T = 1/2$,
(b) $\kappa = m\pi + \pi/2$, L even: $T = 1$,
(c) $\kappa = m\pi$: $T = 1/(1 + L^2)$,
(d) $\kappa = m\pi/L$: $T = 1$,

for integer m. We will refer to the cases when $T = 1$ as transmission resonances. They occur when $\sin L\kappa = 0$. On the other hand, one can see from Eq. (65) that the S-matrix has poles when Eq. (36) is satisfied. Hence the poles of the S-matrix determine the eigenstates of the open system.

(2) In the exponential case, when $\cos 2(\beta - \omega) > 0$, we have $|\chi_\pm|^2 \geq 1$, and $\chi_+ \chi_-^* = 1$, so that $|\chi_-| = \frac{1}{|\chi_+|}$. Then the transmission and reflection coefficients are

$$R = \frac{(|\chi_+|^L - |\chi_-|^L)^2}{(|\chi_+|^L - |\chi_-|^L)^2 + (|\chi_+| - |\chi_-|)^2} \tag{69}$$

$$\approx 1 - |\chi_-|^{2(L-1)} \approx 1, \tag{70}$$

$$T = \frac{(|\chi_+| - |\chi_-|)^2}{(|\chi_+|^L - |\chi_-|^L)^2 + (|\chi_+| - |\chi_-|)^2} \tag{71}$$

$$\approx |\chi_-|^{2(L-1)} \approx 0. \tag{72}$$

4.3.1. *Density profile in the steady state*

As mentioned above, the oscillatory case provides some interesting structures, illustrating the interference between waves traveling to the right and left along the chain. The algebra is tedious but straightforward, and we don't reproduce it here, merely stating the final results. Appendix A contains some formulas involving expression z_n useful for the following calculations.

The wave function in the steady state is

$$\Psi^+(n) = \frac{e^{-i\alpha(n+1)}}{z_L}[z_{L-n-1}\Psi^+(-1) - e^{i\alpha L}e^{i(\alpha - \pi\varphi_p)}\sin(n+1)\kappa\,\Psi^-(L)],$$

$$\Psi^-(n) = \frac{e^{i\alpha(L-n)}}{z_L}[-e^{-i\alpha L}e^{i(\alpha - \pi\varphi_q)}\sin\kappa(L-n)\,\Psi^+(-1) + z_n\Psi^-(L)].$$

We introduce the probability densities, ϱ_L and ϱ_R from the left and right leads, respectively, in terms of the corresponding wave functions, by writing $\Psi^+(-1) = \sqrt{\varrho_L}$, $\Psi^-(L) = \sqrt{\varrho_R}e^{i\eta}$, where η denotes a relative phase between the wave functions at the two ends. Then, introducing the angle $\varphi = \pi(\varphi_q - \varphi_p)/2 + \alpha L + \eta$, we obtain the total probability density at cell n

$$\varrho(n) = \frac{\sin^2(L-n-1)\kappa + \sin^2(L-n)\kappa + \sin^2\kappa}{|z_L|^2}\varrho_L + \frac{\sin^2\kappa n + \sin^2\kappa(n+1) + \sin^2\kappa}{|z_L|^2}\varrho_R$$

$$+ i\frac{\sqrt{\varrho_L\varrho_R}}{|z_L|^2}\left\{\sin(L-n)\kappa\,[z_n e^{i\varphi} - z_n^* e^{-i\varphi}] - \sin(n+1)\kappa\,[z_{L-n-1}^* e^{i\varphi} - z_{L-n-1}e^{-i\varphi}]\right\}$$

$$= \frac{\sin^2(L-n-1)\kappa + \sin^2(L-n)\kappa + \sin^2\kappa}{|z_L|^2}\varrho_L + \frac{\sin^2\kappa n + \sin^2\kappa(n+1) + \sin^2\kappa}{|z_L|^2}\varrho_R$$

$$+2\frac{\sqrt{\varrho_L\varrho_R}}{|z_L|^2}\left\{\sin(L-n)\kappa\,r_n\sin(\varphi+\varphi_n)+\sin(n+1)\kappa\,r_{L-n-1}\sin(\varphi+\varphi_{L-n-1})\right\}.$$

At resonance $(\kappa=m\pi/L)$ it takes form

$$\varrho(n)=\left(1+\frac{\sin^2\kappa n+\sin^2\kappa(n+1)}{\sin^2\kappa}\right)(\varrho_L+\varrho_R) \tag{73}$$

$$+2\frac{\sqrt{\varrho_L\varrho_R}}{\sin^2\kappa}\cos m\pi[\sin(n+1)\kappa\,r_{n+1}\sin(\varphi+\varphi_{n+1})+\sin n\kappa\,r_n\sin(\varphi+\varphi_n)].$$

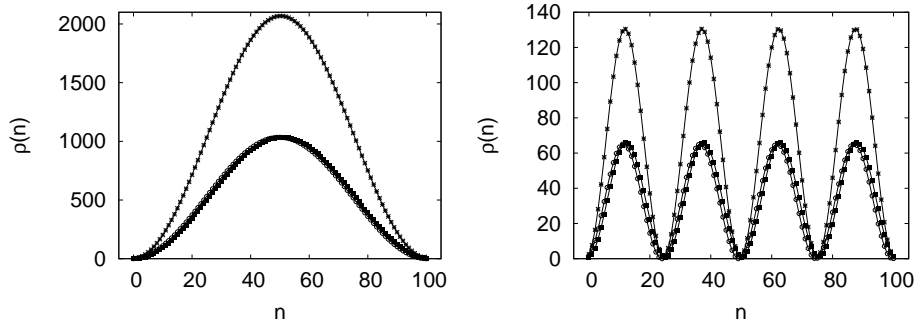Figure 9 shows this solution (crosses) together with the probability density of the

Fig. 9.   Profile of the probability density in the steady state for the smallest and the fourth resonances $\kappa=k\pi/L$ with $k=1,4$ (stars). Also shown is the probability density of the bottom (full boxes) and the top states (open circles). We took $\varrho_L=0.1,\varrho_R=0.9,\eta=0$. The horizontal axis range is $[-5,105]$.

"plus" states (open circles) and the "minus" states (closed squares). For the smallest resonance $(k=1)$ the probability distribution achieves maximum around $n=L/2$ where it is approximately $2L^2/\pi^2$ for $\varphi=\pi/2$.

These results are clearly connected to the slow probability escape $\propto 1/L^3$. To understand them consider a plane wave coming from the left with a resonant frequency going through the open quantum multibaker. Thus at every time step we inject the same density inside. The wave travels ballistically inside and when it reaches the end is mostly reflected, partially transmitted. Due to the fast motion inside and slow decay the density accumulates in the multibaker and reaches the steady state when the escape on the right balanced the injection on the left. The probability density of the resulting standing wave is given by Eq. (73). This result is very striking in comparison with the linear profile of probability density observed in the classical case[69,74,187].

Finally let us observe that in the steady state the current (28) is given by

$$J_{n-1|n}=\frac{1}{|z_L|^2}\left\{\sin^2\kappa(\varrho_L-\varrho_R)+2\sqrt{\varrho_L\varrho_R}\sin\varphi\sin\kappa\sin L\kappa\right\}.$$

Thus it is independent of the position in the chain, as for the eigenstates. In the resonant case, when $\kappa=m\pi/L$ this further simplifies to $J_{n-1|n}=\varrho_L-\varrho_R$.

4.3.2. *Relaxation to steady states*

The approach to the steady state can be conveniently studied as a spectral problem: the evolution equations for the quantum multibaker with two waves scattering from left and right can be written as

$$\widehat{\Psi}(t) = \widehat{\mathbf{M}}_L \widehat{\Psi}(t-1) + \Phi, \tag{74}$$

where $\widehat{\Psi}(t) := e^{-i\omega t}\Psi(t)$. $\widehat{\mathbf{M}}_L$ is the matrix representation of the open multibaker propagator satisfying

$$\begin{bmatrix} \widehat{\Psi}^+(n,t+1) \\ \widehat{\Psi}^-(n,t+1) \end{bmatrix} = e^{-i\omega} \begin{bmatrix} B^+_+(n) \ B^+_-(n) \\ B^-_+(n) \ B^-_-(n) \end{bmatrix} \begin{bmatrix} \widehat{\Psi}^+(n-1,t) \\ \widehat{\Psi}^-(n+1,t) \end{bmatrix}, \tag{75}$$

for $1 \leq n \leq L-2$, while at the boundary

$$\widehat{\Psi}^+(0,t+1) = e^{-i\omega}B^+_-(0)\widehat{\Psi}^-(1,t),$$
$$\widehat{\Psi}^-(0,t+1) = e^{-i\omega}B^-_-(0)\widehat{\Psi}^-(1,t),$$
$$\widehat{\Psi}^+(L-1,t+1) = e^{-i\omega}B^+_+(L-1)\widehat{\Psi}^+(L-2,t),$$
$$\widehat{\Psi}^-(L-1,t+1) = e^{-i\omega}B^-_+(L-1)\widehat{\Psi}^+(L-2,t).$$

Vector Φ denotes the steady state boundary conditions: $\Phi = [\Phi^+(0), \Phi^-(0), \ldots, \Phi^+(L-1), \Phi^-(L-1)]^T$, where

$$\Phi^+(0) = e^{-i\omega}B^+_+(0)\Phi^+(-1),$$
$$\Phi^-(0) = e^{-i\omega}B^-_+(0)\Phi^+(-1),$$
$$\Phi^+(L-1) = e^{-i\omega}B^+_-(L-1)\Phi^-(L),$$
$$\Phi^-(L-1) = e^{-i\omega}B^-_-(L-1)\Phi^-(L),$$

$\Phi^\pm(n) = 0$ otherwise. The solution to this simple affine problem is

$$|\widehat{\Psi}(t)\rangle = \sum_{\lambda_k} \frac{1-\lambda_k^t}{1-\lambda_k}|\varphi_k\rangle\langle\varphi_k|\Phi\rangle + \sum_{\lambda_k} \lambda_k^t|\varphi_k\rangle\langle\varphi_k|\widehat{\Psi}(0)\rangle, \tag{76}$$

where λ_k are the ω-dependent eigenvalues of $\widehat{\mathbf{M}}_L$ and the $|\varphi_k\rangle$ are the corresponding eigenvectors. In particular, if at time 0 the system is empty, $\widehat{\Psi}(0) = 0$, then the solution is

$$|\widehat{\Psi}(t)\rangle = \sum_{\lambda_k} \frac{1-\lambda_k^t}{1-\lambda_k}|\varphi_k\rangle\langle\varphi_k|\Phi\rangle. \tag{77}$$

The steady state is the time invariant part of the above solution

$$|\widehat{\Psi}\rangle = \sum_{\lambda_k} \frac{1}{1-\lambda_k}|\varphi_k\rangle\langle\varphi_k|\Phi\rangle. \tag{78}$$

The approach to the steady state is given by the eigenvalues of the open multibaker (38), thus it is as slow as the escape of probability density, which is consistent with the accumulation of large probability density in the system. Note that the distribution of the absolute values of the eigenvalues of $\widehat{\mathbf{M}}_L$ is ω independent, yet the steady state solution does depend on ω.

4.4. *Mean square displacement*

4.4.1. *Introduction*

The usual approach to classical and quantum transport is through the linear response theory[129,163,213] where one considers the response of the system to a small perturbation of the dynamics due to the external field. This leads to the formulas for transport coefficients involving integrals of various autocorrelation functions. We have used a similar approach to study the transport of a quantum particle moving on a lattice according to a "potential" which classically leads to random walk type of motion. In this case there is no external field, thus we cannot use linear response approach directly. Instead, we proceed analogously as in the classical case. To measure the diffusion of an ensemble of classical particles we use the mean square displacement, which is $\langle (x_t - x_0)^2 \rangle_\varrho$, where ϱ is the initial ensemble which can be localized or uniform (equilibrium ensemble). Since it is not meaningful to speak of a trajectory of a quantum particle, we use the formula $(\Delta x)_t^2 := \langle \Psi | (\hat{x}_t - \hat{x}_0)^2 | \Psi \rangle$ for the mean square displacement (MSD) of the quantum particle. Here $\hat{x}_t$ is the position operator in Heisenberg representation. In Schrödinger representation this formula takes the form

$$(\Delta x)_t^2 = \langle x^2 \rangle_t + \langle x^2 \rangle_0 - 2\Re \int d\Phi \, \langle \Psi_t | x | \Phi_t \rangle \langle \Phi | x | \Psi \rangle, \tag{79}$$

where $\langle A \rangle_t := \langle \Psi_t | A | \Psi_t \rangle$. To get a better feeling for this quantity and to compare it to other measures of "spread" which are used to characterize the dynamics of quantum walks, consider a simple example. Take a Gaussian wave-packet initially localized at ξ with spread Δx moving with average momentum κ:

$$\Psi(x,t) = \left[\sqrt{2\pi} \left(\Delta x + \frac{i\hbar t}{2m\Delta x} \right) \right]^{-\frac{1}{2}} \exp\left[-\frac{(x - \xi - \frac{\kappa t}{m})^2}{4\Delta x(\Delta x + \frac{i\hbar t}{2m\Delta x})} + \frac{i\kappa}{\hbar} \left(x - \frac{\kappa t}{2m} \right) \right]. \tag{80}$$

Thus $\langle x \rangle_0 \equiv \langle \Psi_0 | x | \Psi_0 \rangle = \xi$, $\langle p \rangle_0 = \kappa$, $\langle x^2 \rangle_0 - \langle x \rangle_0^2 = (\Delta x)^2$, $\langle (\Delta p)^2 \rangle_0 = \left(\frac{\hbar}{2\Delta x} \right)^2$. Since the motion is free, the center of motion moves with the average velocity $\langle x \rangle_t \equiv \langle \Psi_t | x | \Psi_t \rangle = \xi + \kappa t/m$, or $\langle x \rangle_t - \langle x \rangle_0 = \kappa t/m$. On the other hand, due to the spread in momenta, the wave-packet spreads ballistically: $(\Delta x_t)^2 \equiv \langle x^2 \rangle_t - \langle x \rangle_t^2 = (\Delta x)^2 + (\frac{\hbar t}{2m\Delta x})^2 = (\Delta x)^2 + (\frac{\Delta p}{2m} t)^2$. It is straightforward to evaluate formula (79) for the wavepacket (80):

$$(\Delta x)_t^2 = |z_t - z_0 e^{-i\omega t}|^2 + |x_t - x_0 e^{-i\omega t}|^2,$$

where $z_t = \Delta x + \frac{i\hbar t}{2m\Delta x}$, $x_t = \langle x \rangle_t = \xi + \kappa t/m$, and $\omega = \frac{\kappa^2}{2m\hbar}$. Therefore, the mean square displacement indicates the summary effect of transport due to the motion of the center of the wavepacket and of the spread of the wave-packet due to the distribution of momenta. For large times we have

$$(\Delta x)_t^2 \approx \left(\frac{\kappa t}{m} \right)^2 + \left(\frac{\hbar t}{2m\Delta x} \right)^2.$$

Both contributions are ballistic but the coefficients are different because of their different causes.

4.4.2. *Mean square displacement for quantum multiplexer maps*

To calculate the mean square displacement for the quantum multiplexer map we use the operators $\mathbf{r}$ and $\mathbf{v} := \mathbf{M}^\dagger \mathbf{r} \mathbf{M} - \mathbf{r}$, which represent the position of the particle on the lattice and its velocity, respectively. Explicitly,

$$\mathbf{r} = \sum_{n,\varepsilon} n \mathbb{I}_{s_\varepsilon} \otimes |n,\varepsilon\rangle\langle n,\varepsilon|, \tag{81}$$

$$\mathbf{v} = \sum_{n,\varepsilon} \varepsilon \mathbb{I}_{s_\varepsilon} \otimes |n,\varepsilon\rangle\langle n,\varepsilon|, \tag{82}$$

(see Appendix B). We use here periodic boundary conditions, therefore we make the velocity operator periodic, so that (81) and (82) holds also for the sites $n = 0, L-1$. An identical form for the velocity occurs in the classical multibaker map as well[46].

Then the mean square displacement takes form

$$\langle (\Delta \mathbf{r})^2(t) \rangle_\Psi = \langle (\sum_{\tau=0}^{t-1} \mathbf{v}_\tau)^2 \rangle_\Psi = \sum_{\tau_1,\tau_2=0}^{t-1} \langle \mathbf{v}_{\tau_1} \mathbf{v}_{\tau_2} \rangle_\Psi, \tag{83}$$

where $\langle A \rangle_\Psi := \langle \Psi | A | \Psi \rangle = \mathrm{Tr}\,(|\Psi\rangle\langle\Psi|A)$. The result depends on the initial state. To characterize the distribution of possible results we calculate its average over all the initial states. This average is our central quantity of interest, the equilibrium mean square displacement

$$\langle (\Delta r)^2(t) \rangle = \sum_{\tau_1,\tau_2=0}^{t-1} \langle \mathbf{v}_{\tau_1} \mathbf{v}_{\tau_2} \rangle, \tag{84}$$

where $\langle A \rangle := \mathrm{Tr}\,(\varrho_{\mathrm{eq}} A) = \mathrm{Tr}\,(A)/LN$. Time invariance of the equilibrium state $\varrho_{\mathrm{eq}} = \mathbb{I}_{NL}/(LN)$ implies invariance of the velocity autocorrelation function $C_{\tau_1,\tau_2} := \langle \mathbf{v}_{\tau_1} \mathbf{v}_{\tau_2} \rangle = C_{\tau_1-\tau_2,0} = C_{0,\tau_1-\tau_2} \equiv C_{\tau_1-\tau_2}$. Thus we can write

$$\langle (\Delta \mathbf{r})^2(t) \rangle = \sum_{\tau=0}^{t-1} C_0 + 2 \sum_{\tau_1 > \tau_2 = 0}^{t-1} C_{\tau_1-\tau_2} = C_0 t + 2 \sum_{\tau=1}^{t-1} (t-\tau) C_\tau. \tag{85}$$

where now

$$C_\tau := \langle \mathbf{v}_\tau \mathbf{v}_0 \rangle = \langle \mathbf{M}^{\dagger\tau} \mathbf{v} \mathbf{M}^\tau \mathbf{v} \rangle. \tag{86}$$

Therefore the mean square displacement can be written as the sum of time correlations of the velocity, just as in the classical case, but the difference in dynamics will lead to important differences in its time development. Using the eigenstates of the quantum multibaker we can further write the velocity autocorrelation function as

$$C_\tau = \frac{1}{LN} \sum_{j,k} |\mathbf{v}_{jk}|^2 e^{i(\varphi_j - \varphi_k)\tau}. \tag{87}$$

We can now write the mean square displacement as

$$\langle (\Delta \mathbf{r})^2(t) \rangle = C_0 t + t(t-1) \frac{1}{LN} \sum_j |\mathbf{v}_{jj}|^2 + \frac{4}{LN} \sum_{j>k} |\mathbf{v}_{jk}|^2 \sum_{\tau=1}^{t-1} \tau \Re e^{i(\varphi_j - \varphi_k)(t-\tau)} \tag{88}$$

$$= \frac{1}{LN} \sum_{j,k} |\mathbf{v}_{jk}|^2 \frac{\sin^2 \frac{(\varphi_j - \varphi_k)t}{2}}{\sin^2 \frac{\varphi_j - \varphi_k}{2}}. \tag{89}$$

Whenever two eigenphases φ_j, φ_k are equal, the contribution to the sum from $\frac{\sin^2 \frac{(\varphi_j - \varphi_k)t}{2}}{\sin^2 \frac{\varphi_j - \varphi_k}{2}}$ must be replaced by t^2.

4.4.3. *General properties of equilibrium mean square displacement*

Using formulas (88) and (89) it is easy to see that the time-dependent mean square displacement for any quantum multiplexer map has to satisfy

(1) $\langle (\Delta \mathbf{r})^2(0) \rangle = 0$,
(2) $\langle (\Delta \mathbf{r})^2(1) \rangle = C_0$,
(3) $0 \leq \langle (\Delta \mathbf{r})^2(t) \rangle \leq C_0 t^2$.

In fact, these results are true in both quantum and classical case. Moreover, it is possible to find local dynamics which realize both of the extremal cases classically and quantum mechanically. As an example consider dyadic multiplexers. As the local scattering map take a right-left exchange operator, defined classically by

$$B(n, x, y) := \begin{cases} (n, x + 1/2, y), & \text{for } 0 \leq x < 1/2, \\ (n, x - 1/2, y), & \text{for } 1/2 \leq x < 1, \end{cases}$$

and quantum mechanically by

$$B := \begin{bmatrix} \mathbb{O} & \mathbb{I} \\ \mathbb{I} & \mathbb{O} \end{bmatrix}.$$

Then the particle jumps between two neighboring sites, which leads to the mean square displacement having values 0 for even and 1 for odd times.

On the other hand, taking identity for the local operator, we induce trivial ballistic motion: particle starting in the state going initially to the right will keep on going to the right, which leads to ballistic transport:

$$\langle (\Delta \mathbf{r})^2(t) \rangle = t^2.$$

Therefore, we see that translational invariance of the coupling operator T allows, in principle, for large asymptotic freedom:

$$\langle (\Delta \mathbf{r})^2(t) \rangle \propto t^\alpha,$$

where $0 \leq \alpha \leq 2$ [d]. An interesting question is, what behavior can be realized in practice. While no constraints seem to be imposed on the classical level, the structure of the quantum mean square displacement, Eq. (89), suggests that for fixed $\hbar$ only $\alpha = 0$ or $\alpha = 2$ are viable. One of the questions it raises is what conditions

---

[d]A more precise statement is: there exists a constant $\alpha \in [0, 2]$ such that $\lim_{t \to \infty} \langle (\Delta \mathbf{r})^2(t) \rangle / t^\beta = \infty$ for $\beta < \alpha$, and $\lim_{t \to \infty} \langle (\Delta \mathbf{r})^2(t) \rangle / t^\beta = 0$ for $\beta > \alpha$.

need to be imposed on the internal dynamics so that the semi-classical limit leads to anomalous diffusion $\alpha \neq 1$. Can such behavior be obtained for infinite length regular quantum multiplexer maps? Random Matrix Theory results for regular quantum multiplexer maps [209,210] (Section 4.4.4) suggest that internal fully chaotic dynamics (mixing) of the classical map implies generically diffusion. We are thus led to believe, that anomalous diffusion can arise in semi-classical limit in systems with partially chaotic, partially integrable internal dynamics. Similar observations were made often before in the context of different types of systems and transport in phase space as opposed to the transport in real space, which we discuss here. More precise results require further study.

For a related classical discrete dynamical system one can show the diffusive character of the dynamics in a rather general case [134e]. Consider dynamics generated by $\varphi : \mathbb{R} \to \mathbb{R}$, and an observable $f : \mathbb{R} \to \mathbb{R}$, for instance coarse position $r \equiv [x]$. The spectral function

$$S(\omega) = \frac{1}{2\pi} \sum_{t=-\infty}^{+\infty} e^{-i\omega t} C(t)$$

is the Fourier transform of the correlation function $C(t) = \langle (f \circ \varphi^t - \langle f \rangle)(f - \langle f \rangle) \rangle$. Then the variance of the displacement can be written as

$$\sigma_n^2 = \left\langle \left[\sum_{k=0}^{n-1} f(\varphi^k X_0) - n\langle f \rangle \right]^2 \right\rangle = \int_{-\pi}^{+\pi} \left(\frac{\sin \frac{\omega n}{2}}{\sin \frac{\omega}{2}} \right)^2 S(\omega) \, d\omega.$$

One can show, that if $\sum_t |tC(t)| < \infty$, then $\sigma_n^2 = 2\pi n S(0) + O(n^0)$, that is the mean square displacement grows diffusively.

4.4.4. *Mean square displacement in the regular multiplexer map*

In case of the regular quantum multiplexer map we can simplify the calculations of the velocity autocorrelation function reducing it to the trace over states in a single cell (Appendix C)

$$C_\tau = \frac{1}{LN} \text{Tr} \left[\mathbf{M}^{\dagger\tau} \mathbf{v} \mathbf{M}^\tau \mathbf{v} \right] = \frac{1}{N} \langle \text{Tr} \left[\tilde{B}^{\dagger\tau} v \tilde{B}^\tau v \right] \rangle_\sim, \tag{90}$$

where $v = \sum_\varepsilon \varepsilon \mathbb{I}_{s_\varepsilon} \otimes |\varepsilon\rangle\langle\varepsilon|$ is the velocity operator $\mathbf{v}$ reduced to a single cell and $\langle f(\tilde{B}) \rangle_\sim := \frac{1}{L} \sum_{k=0}^{L-1} f(B_k)$ is the average over all the modified local operators (11) for the given length. Let us denote the spectrum of a modified local operator $\tilde{B}$ by φ_j and its eigenvectors by $|j\rangle$, that is $\tilde{B}|j\rangle = \exp(i\varphi_j)|j\rangle$. The matrix elements of v in this basis satisfy

$$\sum_{j,k} |v_{jk}|^2 = \text{Tr } v^2 = \sum_\varepsilon \varepsilon^2 s_\varepsilon = \sum_j |v_{jj}|^2 + \sum_{j>k} 2|v_{jk}|^2. \tag{91}$$

---

[e]We are grateful to P. Gaspard for bringing this result to our attention.

With these results we can simplify formula (87) for the velocity autocorrelation as

$$C_\tau = \frac{1}{N}\langle \sum_{j,k} |v_{jk}|^2 e^{i(\tilde{\varphi}_j - \tilde{\varphi}_k)\tau}\rangle_\sim. \tag{92}$$

and formulas (88) and (89) for the mean square displacement

$$\langle (\Delta \mathbf{r})^2(t)\rangle = C_0 t + \frac{t(t-1)}{N}\langle \sum_j |v_{jj}|^2\rangle_\sim + \frac{4}{N}\langle \sum_{j>k} |v_{jk}|^2 \sum_{\tau=1}^{t-1} \tau \Re e^{i(\varphi_j - \varphi_k)(t-\tau)}\rangle_\sim \tag{93}$$

$$= \frac{1}{N}\langle \sum_{j,k} |v_{jk}|^2 \frac{\sin^2 \frac{(\tilde{\varphi}_j - \tilde{\varphi}_k)t}{2}}{\sin^2 \frac{\tilde{\varphi}_j - \tilde{\varphi}_k}{2}}\rangle_\sim. \tag{94}$$

We see that there is typically a ballistic contribution coming from diagonal and possibly some degenerate terms. The other contributions are oscillatory and usually negligible in the long time limit. The final result depends on the particular local quantum operator B employed.

In general, it is not easy to evaluate expression (94) analytically, especially for large N, and one has to resort to numerical methods. If we ask what are generic transport properties of quantum multiplexers we may imagine choosing operator B randomly from some ensemble of unitary operators satisfying appropriate symmetry constraints[95,144,164,183]. Averaging out Eq. (94) over an appropriate ensemble we obtain a result characterizing typical systems from a given symmetry class[209,210]. We assume the distribution of matrix elements is independent of the distribution of elements of eigenvectors[95,131]). Using Eq. (91) one sees that the ensemble average of the mean square displacement takes the form

$$\langle\langle(\Delta \mathbf{r})^2\rangle\rangle = t + t(t-1)\langle|v_{jj}|^2\rangle + 2(N-1)\langle|v_{j\neq k}|^2\rangle \sum_{n=1}^{t-1}(t-n)\langle e^{i\alpha n}\rangle. \tag{95}$$

Straightforward calculation[210] gives $\langle|v_{jj}|^2\rangle = k/(N+k)$, where $k = 1$ for CUE, and 2 for COE. Averaging Eq. (91), we obtain $\langle|v_{jj}|^2\rangle + (N-1)\langle|v_{j\neq k}|^2\rangle = 1$ and thus $\langle|v_{j\neq k}|^2\rangle = N/[(N+k)(N-1)]$.

Calculation of the average value of the exponential factor $\exp[i(\varphi_j - \varphi_k)n]$ involves the expression for the pair correlation function $R(\varphi_j, \varphi_k)$ in the two ensembles

$$\langle e^{[i(\varphi_i - \varphi_k)n]}\rangle = \int_0^{2\pi}\int_0^{2\pi} d\varphi_j \, d\varphi_k \, e^{[i(\varphi_i - \varphi_k)n]} \frac{R(\varphi_j, \varphi_k)}{N(N-1)}.$$

Using the known formulas for correlation functions[144] one obtains

$$\langle e^{[i(\varphi_j - \varphi_k)n]}\rangle_{CUE} = \begin{cases} 1 & \text{for } n = 0 \\ \frac{n-N}{N(N-1)} & \text{for } n < N, \\ 0 & \text{for } n \geq N. \end{cases} \tag{96}$$

for the unitary ensemble, and

$$\langle e^{[i\alpha\tau]}\rangle_{COE} = \begin{cases} 1 & \text{for } \tau = 0 \\ \frac{1}{N(N-1)}[-N + 2\tau[f(\frac{N}{2}+\tau) - f(\frac{N}{2})]] & \text{for } 0 < \tau < N, \\ \frac{1}{N(N-1)}[-N + 2\tau[f(\frac{N}{2}+\tau) - f(\tau-\frac{N}{2})]] & \text{for } \tau \geq N. \end{cases} \quad (97)$$

for the orthogonal ensemble. Here $f(T)$ is defined by

$$f(T) := \sum_{k=1}^{T} \frac{1}{2k-1} = 1 + \frac{1}{3} + \ldots + \frac{1}{2T-1}. \quad (98)$$

This function has at most a logarithmic dependence on its upper limit for large T. Then the evaluation of $\langle\langle(\Delta r)^2(t)\rangle\rangle$ is straightforward and can be written as

$$\langle(\Delta r)^2(t)\rangle = \begin{cases} t + \frac{t(t-1)}{N+k}\left[k - 1 + \frac{t-2}{3(N-1)}\right] + (k-1)\delta_< & \text{for } t \leq N, \\ \frac{k}{N+k}t^2 + \frac{N}{3} - \frac{N(k-1)}{3(N+k)} + (k-1)\delta_> & \text{for } t > N. \end{cases} \quad (99)$$

Here $\delta_{<,>}$ are small corrections to the explicit formulae that have to be evaluated numerically; note that they disappear in the CUE result. Note that the "super-ballistic" t^3 term only occurs for $t \leq N$, where it is typically less than or on the order of the linear term, t.

These results are shown in Figure 10 for $N = 200$. The COE results are two close curves, where the higher is the result given in Eq. (99) for $k = 2$, while in the lower curve the corrections $\delta_{<,>}$ have been neglected. Three asymptotic estimates $t, t^2/N, 2t^2/N$ are also plotted. Inset shows the region $t = 100$ to $t = 300$ where the differences between the two COE results are most pronounced. We observe that RMT average leads to classical diffusion as the short-time prediction in both cases, the CUE average being "more classical". It is worth emphasizing that the classical behavior persists up to the Heisenberg times $\sim h^{-1} = N$ rather than the Ehrenfest time $\sim \ln h^{-1} = \ln N$. On the other hand, for times longer than the Heisenberg time we observe ballistic motion. The ballistic coefficient is proportional to the effective Planck constant therefore it disappears in the semi-classical limit.

In other words, fixing the time and performing semi-classical limit ($h \to 0 \equiv N \to \infty$) we obtain $\langle(\Delta r)^2(t)\rangle = t$, which is the classical result relevant for both the classical multi-baker and the 1D random walk modeled by the classical system. Fixing the Planck constant ($N = const$) and performing long time limit we observe $\langle(\Delta r)^2(t)\rangle = kt^2/N$, which is reflection of the crystal-like structure of the system.

Figure 11 shows the comparison of these predictions with numerical results. For every choice of phases φ_q, φ_p defining the quantization we have checked, for sufficiently large N and L ($N > 100$ and $L > 10$ seems already good enough) the evaluated formula (93) gives results between the COE and CUE predictions. Figure 11 shows the results for the Balazs-Voros phase[11]s ($\varphi_q = \varphi_p = 0$) (in the Saraceno case[152,176] ($\varphi_q = \varphi_p = 0.5$) they are almost identical), and for an example "generic" phases ($\varphi_q = 0.61, \varphi_p = 0.13$). The observed deviation from strict RMT
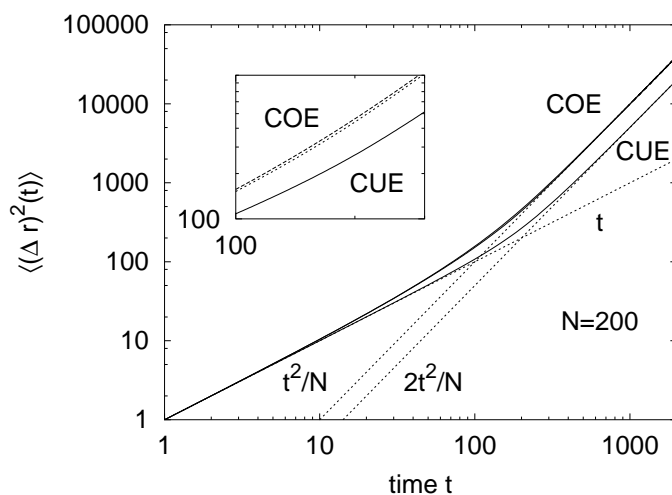
Fig. 10.   Log-log plot of the ensemble averages of the mean square displacement using RMT for $N = 200$. Both CUE and COE results are plotted. The COE results are the two close curves, where the higher is the result given in Eq. (99) for $k = 2$, while in the lower curve the corrections $\delta_{<,>}$ have been neglected. Three asymptotic estimates $t, t^2/N, 2t^2/N$ are also plotted. Inset shows the region $t = 100$ to $t = 300$ where the differences between the two COE results are most pronounced.
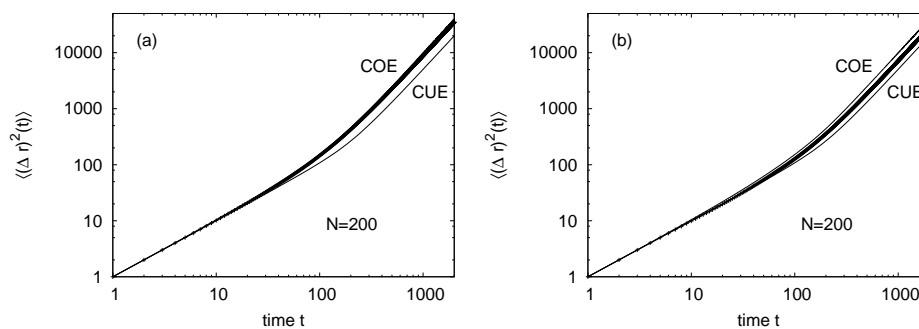

Fig. 11.   Comparison of RMT estimates with the numerical evaluation of the formula (93) for the regular m.s.d. in case of quantum multibakers with a) Balazs-Voros phases, b) "generic" case ($\varphi_q = 0.61, \varphi_p = 0.13$). Plots are in double logarithmic scale; $N = 200$, $L = 100$.

predictions is the result of the spectral properties of quantum baker maps which are not exactly consistent with random matrix theory [132,152].

34   *Daniel K. Wójcik*

4.5. *Velocity autocorrelation functions for quantum multiplexer maps*

Let us look closer at the connection between the velocity autocorrelation function C_τ and the mean square displacement (92). Writing

$$\langle(\Delta\mathbf{r})^2(t)\rangle = (C_0 + 2\sum_{\tau=1}^{t-1} C_\tau)t - 2\sum_{\tau=1}^{t-1} \tau C_\tau$$

we observe that

$$\langle(\Delta\mathbf{r})^2(t+1)\rangle - \langle(\Delta\mathbf{r})^2(t)\rangle = C_0 + 2\sum_{\tau=1}^{t} C_\tau = \sum_{\tau=-t}^{t} C_\tau \tag{100}$$

Therefore, the cumulative sum of velocity autocorrelation function determines the properties of the mean square displacement. In particular the following statements are equivalent for times $t > t_0$

(1) localization $\langle(\Delta\mathbf{r})^2(t)\rangle \sim const$ is equivalent to $\sum_{\tau=-t}^{t} C_\tau \sim 0$,
(2) diffusion $\langle(\Delta\mathbf{r})^2(t)\rangle \sim Ct$ is equivalent to $\sum_{\tau=-t}^{t} C_\tau \sim C > 0$,
(3) ballistic transport $\langle(\Delta\mathbf{r})^2(t)\rangle \sim Ct^2$ is equivalent to $\sum_{\tau=-t}^{t} C_\tau \sim Ct$ or in other words $C_\tau \sim C$.

In regular quantum multibaker maps we observe that the velocity autocorrelation functions, depending on the phases φ_q, φ_p, oscillate wildly around curves lying between the RMT averages (Figure 12). These RMT estimates of C_τ can easily be calculated. Assuming independence of the distributions of eigenvectors and eigenvalues as before and using (92) we obtain

$$C_\tau = \frac{1}{N}[N\langle|v_{jj}|^2\rangle + N(N-1)\langle|v_{j\neq k}|^2\rangle\langle e^{i(\varphi_j-\varphi_k)\tau}\rangle] \tag{101}$$

$$= \frac{N\langle e^{i\alpha\tau}\rangle + k}{N + k}. \tag{102}$$

With the help of (96) and (97) we immediately arrive at the RMT estimates of correlation functions

$$C_{\tau,CUE} = \begin{cases} 1 & \text{for } n = 0 \\ \frac{\tau-1}{N^2-1} & \text{for } n < N, \\ \frac{1}{N+1} & \text{for } n \geq N, \end{cases} \tag{103}$$

for the unitary ensemble, and

$$C_{\tau,COE} = \begin{cases} 1 & \text{for } \tau = 0 \\ \frac{N-2+2\tau[f(\frac{N}{2}+\tau)-f(\frac{N}{2})]}{(N-1)(N+2)} & \text{for } 0 < \tau < N, \\ \frac{N-2+2\tau[f(\frac{N}{2}+\tau)-f(\tau-\frac{N}{2})]}{(N-1)(N+2)} & \text{for } \tau \geq N, \end{cases} \tag{104}$$

for the orthogonal case. Figure 12 shows the plots of COE and CUE estimates for $N = 200$. The value at 0 ($C_0 = 1$) is not shown since the difference $C_0 - C_1$ is much
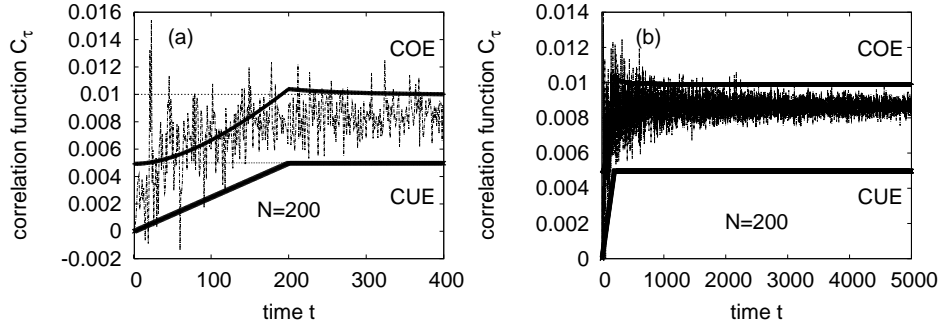
Fig. 12.   Velocity autocorrelation functions C_τ: estimates from random matrix theory for COE and CUE ensembles and the numerically obtained C_τ for regular quantum multibaker maps with $\varphi_q = \varphi_p = 0$; $N = 200$, $L = 10000$. Short time (a) and long time (b) behavior.

greater than the changes in C_τ for $\tau \geq 1$. Substituting these results into (92) leads to previously obtained formulas for the mean square displacement, eq. (99).

Since $f(\frac{N}{2} + \tau) - f(\tau - \frac{N}{2})$ for large τ consists of N terms each of order $(2\tau)^{-1}$ the COE correlation function tends to $2/N$. From the perspective of equation (85), as observed above, the asymptotic residuals $C_\tau \approx k/N$ give rise to the ballistic transport. The ballistic coefficient is given by C_∞. Indeed, for large times we can take C_τ approximately constant and the mean square displacement $\langle (\Delta \mathbf{r})^2(t) \rangle$ is dominated by $C_\tau t^2 = kt^2/N$.

For disordered quantum multibaker maps we observe that the velocity autocorrelation functions C_τ (Figure 13 (a)) can be split into two parts $C_\tau = C_\tau^1 + C_\tau^2$ with the following properties:

(1) $C_\tau^1 = 0$ for $\tau > t_0$,
(2) $\sum_{\tau=-t_0}^{t_0} C_\tau^1 = 0$ which together with (1) implies $\sum_{\tau=-t}^{t} C_\tau^1 = 0$ for $t > t_0$,
(3) $C_\tau^2 = (-1)^\tau C$.

Numerically, assuming this decomposition and the oscillating form of C_τ^2 we observe that C_τ^1 oscillates around 0 for $t > t_0$ (Figure 13 (b)) and the variance of the oscillations decays with the increase of the size of the system or with the number of realizations of finite systems over which we average. This observed structure of C_τ leads to localization. Figure 13 (c) shows the behavior of $\sum_{\tau=-t}^{t} C_\tau$ as a function of time, Figure 13 (d) shows the mean square displacement obtained from this correlation function by application of formula (92). The effect of the observed oscillations of the sum $\sum_{\tau=-t}^{t} C_\tau^1$ is visible in the plot of the mean square displacement in the slightly non-zero slope of its long-time behavior.

5. Other quantum walks

Quantum multibaker maps were proposed as models for the study of the signatures of microscopic classical chaos in quantum transport. As quantizations of classical
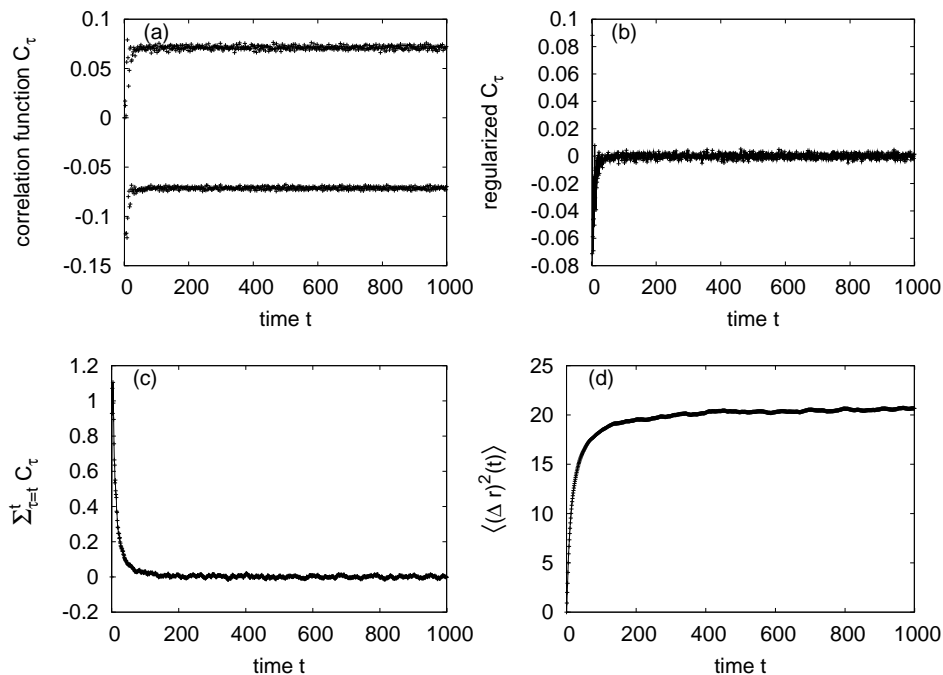
Fig. 13.   (a) Velocity autocorrelation function C_τ for random quantum multibaker map with $N = 2$. The size of the system was $L = 1000$ and average over 32 realizations is shown. (b) Velocity autocorrelation function C_τ^1 renormalized by subtraction of the oscillating part $C_\tau^2 = (-1)^\tau C$, C was taken as the average of $|C_\tau|$ over times $\tau > 20$. (c) Behavior of $\sum_{\tau=-t}^{t} C_\tau$ as a function of time. (d) Mean square displacement obtained from this correlation function by application of formula (92).

multibaker maps, hamiltonian models of one-dimensional random walks on the lattice, they are natural representations of quantum random walks. The studies of quantum walks[2,91], quantum cellular automata[16,125] or quantum lattice gases[184] in recent years are gaining on popularity. While the simplest of these models are close in spirit to Krönig-Penney model[128], the first quantum random walk, often called *Hadamard walk*, was obtained by S. Godoy and S. Fujita[91] by approximating the evolution of special wave packets in Krönig-Penney type potential. Formally similar model was discussed by D. Aharonov, et al.[2], who considered the motion of spin-$\frac{1}{2}$ particles in one dimension, and proposed experimental realization of the walk in the framework of quantum optics.

The same year S. Suzzi and R. Benzi observed[184] that the lattice Boltzman equation can be transformed so as to describe non-relativistic quantum mechanics. Also in 1993 M. Kostin proposed[125] a cellular automaton which in the limit of diminishing spatial and temporal scales reduced to Dirac equation, which was, however, nonunitary. Improved unitary models, which are examples of quantum lattice walks, were proposed a year later by I. Białynicki-Birula[16], as discrete ver-

sions of Weyl, Dirac, and Maxwell equations. In a way, one can consider Feynman's studies of path integrals for Dirac equation another predecessor of lattice quantum walks[62,178].

These models inspired D. Meyer who, in his studies of quantum cellular automata for their possible applications to quantum computing, obtained a model essentially equivalent to the Hadamard walk[145]. This model was later discussed by A. Nayak and A. Vishwanath[149] and — in various veins, for different boundary conditions — by others[6,9,18,122,124,126,156,165]. An early review of these results from quantum algorithmic perspective can be found in[116].

Other variants of lattice quantum walks were also considered, some inspired by optical networks of Törma[194] and including phase shifts in the dynamics[26,101,127,206], some with generalized dynamics (different local operators, or "coins") or in more dimensions[63,93,105,123,138]. Several implementations of quantum walks were proposed using ion traps[195], neutral atoms trapped in optical lattices[50], classical optical systems[21,113], and optical cavities[45,122,175].

Most of these studies were conducted in the framework of quantum information theory, therefore the emphasis was often on possible applications in quantum computing and development of new quantum algorithms. For instance, several quantum-walk based search algorithms were proposed[33,34,180]. Also, since noise, decoherence and measurements disturb the evolution of the system, potentially preventing its intended computational use, the influence of these effects on dynamics and on wave packet transport in quantum walks were studied[25,54,113,117,118,136,167,179].

An interesting application of quantum walks was recently discussed by Oka et al.[153] who studied dielectric breakdown of an electron system driven by strong electric field. The authors mapped the Landau-Zener transition dynamics to a quantum walk with a reflecting boundary corresponding to the ground state and observed a delocalization transition with increasing external field.

While time-discrete quantum walks on lattices dominate the recent literature there are some interesting studies of discrete walks on more general graphs[3,29,180] as well as of continuous time quantum walks[3,32,60,147,148].

Much of the work on lattice quantum walks can easily be reformulated in terms of the multibaker or multiplexer maps. In particular, the map corresponding to the largest possible value of Planck's constant, $h = 1/2$, or equivalently, $N = 2$. To appreciate this connection let us recall the definition of the simplest *Hadamard walk*.

Here one considers a particle walking on a one-dimensional lattice. With every lattice site one associates a state $|n\rangle$, where $n \in \mathbb{Z}$ is the site number. To allow for jumps to neighboring cells the Hilbert space must be enlarged[145]. This is achieved by adding another degree of freedom (a "spin" or a "quantum coin") which can take one of two values, $d = r, l$. Depending on the state of the coin the particle jumps one step right or left. The Hilbert space consists of the product states $|n\rangle \otimes |d\rangle$ and the evolution is described in two steps. One "throws a quantum coin", that is acts

with a unitary operator $\mathbf{H}$ on the "coin" degrees of freedom

$$\begin{pmatrix} |n,r'\rangle \\ |n,l'\rangle \end{pmatrix} = \mathbf{H} \begin{pmatrix} |n,r\rangle \\ |n,l\rangle \end{pmatrix} = \frac{1}{\sqrt{2}} \begin{pmatrix} 1 & 1 \\ 1 & -1 \end{pmatrix} \cdot \begin{pmatrix} |n,r\rangle \\ |n,l\rangle \end{pmatrix}. \tag{105}$$

This step is now coupled to a translation, $\mathbf{T}$ of $|n,r'\rangle$ one unit to the right and, similarly, $|n,l'\rangle$ one unit to the left, as

$$\begin{aligned} \mathbf{T}|n,r\rangle &= |n+1,r\rangle, \\ \mathbf{T}|n,l\rangle &= |n-1,l\rangle. \end{aligned} \tag{106}$$

H is called the *Hadamard gate* in quantum computing literature [151,160], which gives rise to the name *Hadamard walk*. Finally the two operations are combined to form the operator $\mathbf{T} \circ \mathbf{H} = \mathbf{W}$, which describes one step of the Hadamard walk,

$$\begin{aligned} |n,r,t\rangle &= \frac{1}{\sqrt{2}} \left[|n-1,r,t-1\rangle + |n+1,l,t-1\rangle \right], \\ |n,l,t\rangle &= \frac{1}{\sqrt{2}} \left[|n-1,r,t-1\rangle - |n+1,l,t-1\rangle \right]. \end{aligned} \tag{107}$$

These equations are identical to Eq. (6) for $N = 2$ for the special case that the Balazs-Voros phases [11], $\varphi_q = \varphi_p = 0$, are used. Therefore, the multi-baker map and the Hadamard walk are identical, for the Balazs-Voros phases and $N = 2$.

Formally, quantum lattice walks and quantum multiplexer maps discussed in the present article have large overlap. The difference is in the emphasis: in the studies of quantum multibaker maps we are interested in the properties of the whole families of systems parametrized by the dimension of the "coin" Hilbert space with a common semiclassical limit, and in the quantum signatures of chaos of the limiting classical system. The freedom of choice of a particular quantization of local scattering map in the transformation equations allows one to consider a variety of systems including uniform, periodic, quasi-periodic, and random systems, all of which can share the same semiclassical limit. This is typically not considered in the studies of quantum walks. Thus one can find a range of phenomena in quantum multiplexer maps ranging from localization to ballistic motion. Such phenomena show up in many condensed matter systems. Further, the use of a variable Planck constant allows for several channels of motion to be taking place at once, and allows us to treat semiclassical as well as strong quantum versions of these maps. This is what makes the multiplexer maps so appealing for studying exact transport properties of condensed quantum systems.

6. Conclusions and open questions

Recent developments in dynamical systems theory together with the increasing computational power made possible new developments in nonequilibrium statistical mechanics. Two approaches were particularly fruitful, the escape-rate theory

of Gaspard and Nicolis[83] for open hamiltonian systems, and the dynamical thermostats[57,102,174] methods which led to the studies of Sinai-Ruelle-Bowen measures describing extended dissipative systems.

As most of these developments happened for classical systems it was natural to ask if these new results have their counterpart in the quantum case. To carry out such inquiries a new family of systems was introduced[208] called quantum multibaker maps. These models are quantizations of the classical multibaker maps which are deterministic models of simple random walks on the lattice[187]. The understanding of the classical limit as well as of the quantum components (quantum baker maps[11,176]) was very helpful in the analysis of the quantum multibaker maps.

In this article we have reviewed the construction and properties of these quantum maps with space extent presenting a slightly more general framework, which we call quantum multiplexer maps (Section 3.3). To help the reader understand the context of these studies as well as to provide him with some relevant background literature, we have reviewed broadly these new results in nonequilibrium statistical mechanics (Section 1) with special emphasis on the construction and properties of classical multibaker maps (Section 2). In Section 3 we discussed the quantum maps and described the framework of general quantum multiplexer maps. Some known properties of these systems were recalled in Section 4. Since these systems can be considered paradigmatic quantum walks we have also provided some information about the recent developments of related quantum walk models in Section 5.

There are many questions one would like to answer with the help of quantum multiplexer maps. We know that the Pollicott-Ruelle resonances determine the relaxation properties of the classical extended systems to equilibrium or to steady states (Section 1). The resonances for classical multibaker maps are well-known[71,187]. On quantum level the resonances correspond to the poles of analytic continuation of quantum evolution operator. Since quantum multibaker maps come in many variants, notably translationally invariant and completely disordered, with very different transport properties, the question is what are the properties of these poles and how does one recover the Pollicott-Ruelle resonances in the semiclassical limit?

It is conjectured for the classical systems that the source of positive entropy production is the fractality of the measures describing steady states[80,89]. Quantum mechanically steady states cannot be fractals[15,207] for any finite N. Moreover, all the quantum entropies corresponding to Kolmogorov-Sinai entropy are zero for finite systems[5]. This leads to the question if one can define entropy production for quantum systems so that it would be positive, at least semiclassically, and how does one regain the classical result. Also, how does one recover the classical fractality of nonequilibrium steady states?

To go in this direction one needs semiclassical description of models considered here. However, there are no semiclassical studies of quantum multibaker (or other multiplexer) maps yet. Such theory should be possible given the good understanding

of semiclassics of simple quantum maps [19,43,95,96,177]. Can one take into account the lattice distribution of phases parametrizing local quantization?

Many variants of quantum multibaker maps are unexplored, for instance the version with diluted scatterers (Section 3). When the density of the scatterers changes from 1 to 0 we expect a transition from ballistic motion to localization. How does this transition occur? Is it smooth or shall we see a phase transition?

We believe that the models presented in this review can be very useful for understanding the quantum transport and the changes of its character in semiclassical limit from dynamical perspective. We hope that this work will stimulate further research in this direction.

Acknowledgements

Appendix A. Properties of z_n

We list here some useful formulas for expressions involving z_n, eq. (66),

$$z_n = \sqrt{2}\sin n\kappa\, e^{-i(\beta-\omega)} - \sin\kappa(n-1).$$

(1) $z_n = \cos\kappa n \sin\kappa - i\varepsilon\sin n\kappa\sqrt{1+\sin^2\kappa}$, where ε is the sign of $\sin(\beta-\omega)$,
(2) $z_k^* = z_{-k}$,
(3) $z_{k+n}\sin\kappa = z_k z_n + \sin k\kappa \sin n\kappa$,
(4) $\sin(k+n)\kappa\sin\kappa = \sin k\kappa\, z_n^* + \sin n\kappa\, z_k$,
(5) $|z_n|^2 = \sin^2\kappa + \sin^2 n\kappa$.

Proof:

(1) From eq. (64) we have

$$e^{i\kappa} = \sqrt{2}\cos(\beta-\omega) + i\sqrt{-\cos 2(\beta-\omega)}.$$

   Thus $\sqrt{2}\cos(\beta-\omega) = \cos\kappa$ and $\sqrt{2}\sin(\beta-\omega) = \varepsilon\sqrt{1+\sin^2\kappa}$, where ε is the sign of $\sin(\beta-\omega)$. The new formula is obtained upon substitution.
(2) From definition.
(3) From $T^{n+k} = T^n T^k$.
(4) From $T^{n+k} = T^n T^k$.
(5) From (1).

Appendix B. Velocity operator in the general case

Let us write the quantum multiplexer operator in the position basis

$$\mathbf{M} = \sum_n \sum_{\varepsilon_1,\varepsilon_2} B^{\varepsilon_1}_{\varepsilon_2}(n+\varepsilon_2)|n+\varepsilon_2,\varepsilon_1\rangle\langle n,\varepsilon_2|.$$

Then its inverse is

$$\mathbf{M}^\dagger = \sum_m \sum_{\varepsilon_3,\varepsilon_4} D^{\varepsilon_4}_{\varepsilon_3}(m)|m-\varepsilon_4,\varepsilon_4\rangle\langle m,\varepsilon_3|.$$

Here $D^{\varepsilon_4}_{\varepsilon_3}(m)$ are blocks of the inverse local scattering operator $D(n) \equiv B^\dagger(n)$ so that

$$\sum_\varepsilon B^{\varepsilon_2}_{\varepsilon}(n)D^{\varepsilon}_{\varepsilon_1}(n) = \delta_{\varepsilon_2,\varepsilon_1}|n,\varepsilon_2\rangle\langle n,\varepsilon_1|.$$

To obtain velocity operator we need the formula for $\mathbf{M}^\dagger\mathbf{r}\mathbf{M}$, where $\mathbf{r}$ is given by Eq. (81)

$$
\begin{aligned}
\mathbf{M}^\dagger\mathbf{r}\mathbf{M} &= \sum_{n,m}\sum_{\varepsilon_1,\varepsilon_2,\varepsilon_3,\varepsilon_4}(n+\varepsilon_2)D^{\varepsilon_4}_{\varepsilon_3}(m)B^{\varepsilon_1}_{\varepsilon_2}(n+\varepsilon_2)|m-\varepsilon_4,\varepsilon_4\rangle\langle m,\varepsilon_3||n+\varepsilon_2,\varepsilon_1\rangle\langle n,\varepsilon_2|\\
&= \sum_{n,m}\sum_{\varepsilon_1,\varepsilon_2,\varepsilon_3,\varepsilon_4}(n+\varepsilon_2)D^{\varepsilon_4}_{\varepsilon_3}(m)B^{\varepsilon_1}_{\varepsilon_2}(n+\varepsilon_2)\delta_{m,n+\varepsilon_2}\delta_{\varepsilon_1,\varepsilon_3}|m-\varepsilon_4,\varepsilon_4\rangle\langle n,\varepsilon_2|\\
&= \sum_n\sum_{\varepsilon_1,\varepsilon_2,\varepsilon_4}(n+\varepsilon_2)D^{\varepsilon_4}_{\varepsilon_1}(n+\varepsilon_2)B^{\varepsilon_1}_{\varepsilon_2}(n+\varepsilon_2)|n+\varepsilon_2-\varepsilon_4,\varepsilon_4\rangle\langle n,\varepsilon_2|\\
&= \sum_n\sum_{\varepsilon_2,\varepsilon_4}(n+\varepsilon_2)\delta_{\varepsilon_2,\varepsilon_4}|n+\varepsilon_2-\varepsilon_4,\varepsilon_4\rangle\langle n,\varepsilon_2|\\
&= \sum_{n,\varepsilon_2}(n+\varepsilon_2)|n,\varepsilon_2\rangle\langle n,\varepsilon_2|.
\end{aligned}
$$

Therefore

$$\mathbf{v} = \mathbf{M}^\dagger\mathbf{r}\mathbf{M} - \mathbf{r} = \sum_{n,\varepsilon}(n+\varepsilon)|n,\varepsilon\rangle\langle n,\varepsilon| - \sum_{n,\varepsilon}n|n,\varepsilon\rangle\langle n,\varepsilon| = \sum_{n,\varepsilon}\varepsilon|n,\varepsilon\rangle\langle n,\varepsilon|.$$

The above calculation is clearly incorrect at the boundary, however, we use periodic boundary conditions and so we make the velocity operator periodic requiring translational invariance on the circle

$$\mathbf{v} = \sum_{n=0}^{L-1}\sum_\varepsilon \varepsilon|n,\varepsilon\rangle\langle n,\varepsilon|.$$

Observe that the form of the velocity operator is independent of the local operators $B(n)$, as well as of the number of ε subspaces, as long as the multiplexer structure (Section 3.3) is preserved.

Appendix C. Reduction of the calculation of the mean square displacement in translationally invariant case to a single cell

Let us calculate the velocity autocorrelation function of the translationally invariant dyadic quantum multibaker map (16):

$$
\begin{aligned}
C_\tau &= \frac{1}{LN} \mathrm{Tr}[\mathbf{M}^{\dagger\tau} \mathbf{v} \mathbf{M}^\tau \mathbf{v}] \\
&= \frac{1}{LN} \sum_{k,l=0}^{L-1} \sum_{\alpha,\beta=0}^{N-1} \langle k,\alpha | \mathbf{M}^{\dagger n} \mathbf{v} \mathbf{M}^n | l,\beta \rangle \langle l,\beta | \mathbf{v} | k,\alpha \rangle \\
&= \frac{1}{LN} \sum_{k,l=0}^{L-1} \sum_{\alpha,\beta=0}^{N-1} e^{i(\varphi_{l,\beta} - \varphi_{k,\alpha})\tau} |\langle l,\beta | \mathbf{v} | k,\alpha \rangle|^2,
\end{aligned}
$$

where $|k,\alpha\rangle$ are the eigenstates of quantum multibaker operator M corresponding to the wavenumber $\kappa = 2\pi k/L$. Thus $M|k,\alpha\rangle = e^{i\varphi_{k,\alpha}}|k,\alpha\rangle$ and

$$
|k,\alpha\rangle = \sum_{n,\varepsilon} e^{i2\pi kn/L} \tilde{\Psi}_\varepsilon^{k,\alpha} \otimes |n,\varepsilon\rangle,
$$

where $\tilde{\Psi}_\varepsilon^{k,\alpha}$ is an eigenvector of the modified quantum baker map (13) for this wavenumber. Therefore,

$$
\mathbf{v}|k,\alpha\rangle = \sum_{n,\varepsilon} \varepsilon e^{i2\pi kn/L} \tilde{\Psi}_\varepsilon^{k,\alpha} \otimes |n,\varepsilon\rangle,
$$

and

$$
\langle l,\beta | \mathbf{v} | k,\alpha \rangle = \sum_{n,\varepsilon} \varepsilon e^{i2\pi(k-l)n/L} \tilde{\Psi}_\varepsilon^{l,\beta\,\dagger} \tilde{\Psi}_\varepsilon^{k,\alpha} = \tilde{\Psi}^{l,\beta\,\dagger} v \tilde{\Psi}^{k,\alpha} \delta_{k,l}.
$$

Therefore

$$
C_\tau = \frac{1}{LN} \sum_{k=0}^{L-1} \mathrm{Tr}[\tilde{B}_k^{\dagger\tau} v \tilde{B}_k^\tau v], \tag{C.1}
$$

where $\tilde{B}_k$ is the modified quantum baker map (13) for $\kappa = 2\pi k/L$ and v is the velocity operator $\mathbf{v}$ restricted to a single cell.

This simplification can also be performed for other dyadic quantum multiplexer maps and can easily be generalized to more dimensional systems as long as the translational invariance of the lattice is preserved (of course, in more dimensions velocity becomes a vector operator).

References

1. O. Agam. Diagrammatic approach for open chaotic systems. *Phys. Rev. E*, 61:1285–1298, 2000.
2. Y. Aharonov, L. Davidovich, and N. Zagury. Quantum random-walks. *Phys Rev A*, 48(2):1687–1690, 1993.

3. A. Ahmadi, R. Belk, C. Tamon, and C. Wendler. On mixing in continuous-time quantum walks on some circulant graphs. *Quantum Inf. & Comp.*, 3(6):611–618, Nov. 2003.

4. Y. Alhassid. The statistical theory of quantum dots. *Rev. Mod. Phys.*, 72:895, 2000.

5. R. Alicki and M. Fannes. *Quantum dynamical systems*. Oxford Univ. Press, Oxford, 2001.

6. A. Ambainis, E. Bach, A. Nayak, A. Vishwanath, and J. Watrous. One-dimensional quantum walks. In *Proceedings of the 30th Annual ACM Symposium on Theory of Computing*, pages 37–49, New York, 2001. Association for Computing Machinery.

7. P. W. Anderson. Absence of diffusion in certain random lattices. *Phys. Rev.*, 109:1492–1505, 1958.

8. D. Andrieux and P. Gaspard. Fluctuation theorem for transport in mesoscopic systems. *J. Stat. Mech. — Th. and Exp.*, page P01011, 2006.

9. E. Bach, S. Coppersmith, M. P. Goldschen, R. Joynt, and J. Watrous. One-dimensional quantum walks with absorbing boundaries. *Journal of Computer and System Sciences*, 69(4):562–592, 2004.

10. A. Bäcker. Numerical aspects of eigenvalue and eigenfunction computations for chaotic quantum systems. In M. Degli Esposti and S. S. Graffi, editors, *The Mathematical Aspects of Quantum Maps*, volume 618 of *Lecture Notes in Physics*, pages 91–144. Springer Verlag, Berlin, 2003.

11. N. L. Balazs and A. Voros. The quantized baker's transformation. *Ann. Phys.*, 190:1–31, 1989.

12. F. Barra and P. Gaspard. Scattering in periodic systems: from resonanses to band structure. *J. Phys. A*, 32:3357, 1999.

13. C. Beck and F. Schlögl. *Thermodynamics of Chaotic Systems*. Cambridge University Press, Cambridge, UK, 1997.

14. C. W. J. Beenakker. Random-marix theory of quantum transport. *Rev. Mod. Phys.*, 69(3):731, 1997.

15. M. V. Berry. Quantum fractals in boxes. *J. Phys. A-Math. Gen.*, 29:6617–6629, 1996.

16. I. Białynicki-Birula. Weyl, Dirac, and Maxwell equations on a lattice as unitary cellular automata. *Phys. Rev. D*, 49:6920, 1994.

17. G. Birkhoff. *Dynamical systems*. Am. Math. Soc., 1927.

18. P. Blanchard and M. O. Hongler. Quantum random walks and piecewise deterministic evolutions. *Phys. Rev. Let.*, 92(12):120601, Mar. 2004.

19. P. A. Boasman and J. P. Keating. Semiclassical asymptotics of perturbed cat maps. *Proc. R. Soc. London Ser. A-Math. Phys. Sci.*, 449:629–653, 1995.

20. T. Bohr and D. Rand. The entropy function for characteristic exponents. *Physica D*, 25:387, 1987.

21. D. Bouwmeester, I. Marzoli, G. P. Karman, W. Schleich, and J. P. Woerdman. Optical Galton board. *Phys. Rev. A*, 61:61, 1999.

44   *REFERENCES*

22. A. Bouzouina and S. DeBievre. Equipartition of the eigenfunctions of quantized ergodic maps on the torus. *Commun. Math. Phys.*, 178:83–105, 1996.

23. W. Breymann, T. Tel, and J. Vollmer. Entropy balance, time reversibility, and mass transport in dynamical systems. *Chaos*, 8:396–408, 1998.

24. W. G. Breymann, T. Tel, and J. Vollmer. Entropy production for open dynamical systems. *Phys. Rev. Lett.*, 77:2945–2948, 1996.

25. T. A. Brun, H. A. Carteret, and A. Ambainis. Quantum to classical transition for random walks. *Phys. Rev. Let.*, 91(13):130602, 2003.

26. O. Buerschaper and K. Burnett. Stroboscopic quantum walks. quant-ph/0406039, 2004.

27. L. A. Bunimovich. On ergodic properties of nowhere dispersing billiards. *Comm. Math. Phys.*, 65:295, 1979.

28. C. Bustamante, J. Liphardt, and F. Ritort. The nonequilibrium thermodynamics of small systems. *Physics Today*, 58:43–48, July 2005.

29. I. Carneiro, M. Loo, X. B. Xu, M. Girerd, V. Kendon, and P. L. Knight. Entanglement in coined quantum walks on regular graphs. *New Journal of Physics*, 7:156, 2005.

30. N. I. Chernov, G. L. Eyink, J. L. Lebowitz, and Y. G. Sinai. Derivation of Ohm's law in a deterministic mechanical model. *Phys. Rev. Lett.*, 70:2209–2212, 1993.

31. N. J. Chernov, G. L. Eyink, J. L. Lebowitz, and Y. G. Sinai. Steady-state electrical conduction in the periodic Lorentz gas. *Comm. Math. Phys.*, 154:569–601, 1993.

32. A. M. Childs, E. Farhi, and S. Gutmann. An example of the difference between quantum and classical random walks. *Quantum Inf. Process.*, 1:35, 2002.

33. A. M. Childs and J. Goldstone. Spatial search and the Dirac equation. *Phys. Rev. A*, 70(4):042312, Oct. 2004.

34. A. M. Childs and J. Goldstone. Spatial search by quantum walk. *Phys. Rev. A*, 70(2):022314, Aug. 2004.

35. S. Ciliberto and C. Laroche. An experimental test of the Gallavotti-Cohen fluctuation theorem. *J. Phys. IV*, 8:215–219, 1998.

36. E. G. D. Cohen and L. Rondoni. Particles, maps and irreversible thermodynamics. *Physica A*, 306(1-4):117–128, Apr. 2002.

37. G. E. Crooks. Nonequilibrium measurements of free energy differences for microscopically reversible markovian systems. *J. Stat. Phys.*, 90:1481–1487, 1998.

38. G. E. Crooks. Entropy production fluctuation theorem and the nonequilibrium work relation for free energy differences. *Phys. Rev. E*, 60:2721–2726, 1999.

39. F. M. Cucchietti, H. M. Pastawski, and D. A. Wisniacki. Decoherence as decay of the Loschmidt echo in a Lorentz gas. *Phys. Rev. E*, 65:045206, 2002.

40. P. Cvitanović, R. Artuso, R. Mainieri, G. Tanner, and G. Vattay. *Chaos: Classical and Quantum*. Niels Bohr Institute, Copenhagen, 2005. `ChaosBook.org`.

41. S. De Biévre. Quantum chaos: a brief visit. In S. Perez-Esteva and C. Villegas-

Blas, editors, *Second Summer School in Analysis and Mathematical Physics: Topics in Analysis: Harmonic, Complex, Nonlinear, and Quantization*, volume 289 of *Contemporary Mathematics*. AMS, 2001.

42. S. De Bievre and M. D. Esposti. Egorov theorems and equidistribution of eigenfunctions for the quantized sawtooth and baker maps. *Ann. Inst. Henri Poincare-Phys. Theor.*, 69:1–30, 1998.

43. M. B. de Matos and A. M. O. de Almeida. Quantization of Anosov maps. *Ann. Phys.*, 237:46–65, 1995.

44. S. DeBievre, M. D. Esposti, and R. Giachetti. Quantization of a class of piecewise affine transformations on the torus. *Commun. Math. Phys.*, 176:73–94, 1996.

45. T. G. Di, M. Hillery, and M. S. Zubairy. Cavity QED-based quantum walk. *Phys. Rev. A*, 70(3):032304, 2004.

46. J. R. Dorfman. *An introduction to chaos in nonequilibrium statistical mechanics.* Cambridge University Press, Cambridge, 1999.

47. J. R. Dorfman. Fractal structures in the phase space of simple chaotic systems with transport. In P. Garbaczewski and R. Olkiewicz, editors, *Dynamics of dissipation*, volume 597 of *LNP*, pages 193–212. Springer Verlag, 2002.

48. F. Douarche, S. Ciliberto, A. Petrosyan, and I. Rabbiosi. An experimental test of the Jarzynski equality in a mechanical experiment. *Europhys. Lett.*, 70:593–599, 2005.

49. D. Driebe. *Fully Chaotic Maps and Broken Time Symmetry.* Kluwer, Boston, 1999.

50. W. Dur, R. Raussendorf, V. M. Kendon, and H. J. Briegel. Quantum walks in optical lattices. *Phys. Rev. A*, 66(5):052319, 2002.

51. J.-P. Eckmann and D. Ruelle. Ergodic theory of chaos and strange attractors. *Rev. Mod. Phys.*, 57:617–656, 1985.

52. K. Efetov. *Supersymmetry in disorder and chaos.* Cambridge University Press, Camridge, 1997.

53. Y. Elskens and R. Kapral. Reversible dynamics and the macroscopic rate law for a solvable Kolmogorov system: The three bakers' reaction. *J. Stat. Phys.*, 38:1027, 1985.

54. L. Ermann, J. P. Paz, and M. Saraceno. Decoherence induced by a chaotic enviroment: A quantum walker with a complex coin. *Phys. Rev. A*, 73(1):012302, Jan. 2006.

55. M. Esposito and P. Gaspard. Spin relaxation in a complex environment. *Phys. Rev. E*, 68:66113, 2003.

56. D. J. Evans, E. G. D. Cohen, and G. P. Morriss. Probability of 2nd law violations in shearing steady-states. *Phys. Rev. Lett.*, 71:2401–2404, 1993.

57. D. J. Evans and G. Morriss. *Statistical mechanics of non-equilibrium liquids.* Academic Press, London, 1990.

58. D. J. Evans and D. Searles. The fluctuation theorem. *Advances In Physics*, 51:1529–1585, 2002.

46   *REFERENCES*

59. D. J. Evans and D. J. Searles. Equilibrium microstates which generate 2nd law violating steady-states. *Phys. Rev. E*, 50:1645–1648, 1994.
60. E. Farhi and S. Gutmann. Quantum computation and decision trees. *Phys. Rev. A*, 58:915–928, 1998.
61. D. K. Ferry and S. M. Goodnick. *Transport in Nanostructures*. Cambridge University Press, Cambridge, 1997.
62. R. P. Feynman. Space-time approach to non-relativistic quantum mechanics. *Rev. Mod. Phys.*, 20:367–387, 1948.
63. S. Fujiwara, H. Osaki, I. M. Buluta, and S. Hasegawa. Scalable networks for discrete quantum random walks. *Phys. Rev. A*, 72(3):032329, Sept. 2005.
64. G. Gallavotti. Dynamical ensembles equivalence in fluid mechanics. *Physica D*, 105:163–184, 1997.
65. G. Gallavotti and E. G. D. Cohen. Dynamical ensembles in nonequilibrium statistical-mechanics. *Phys. Rev. Lett.*, 74:2694–2697, 1995.
66. G. Gallavotti and E. G. D. Cohen. Dynamical ensembles in stationary states. *J. Stat. Phys.*, 80:931–970, 1995.
67. N. Garnier and S. Ciliberto. Nonequilibrium fluctuations in a resistor. *Phys. Rev. E*, 71:060101, 2005.
68. N. Garnier and D. K. Wójcik. Spatiotemporal chaos: the microscopic perspective. *Phys. Rev. Let.*, to appear, 2006.
69. P. Gaspard. Diffusion, effusion, and chaotic scattering: an exactly solvable Liouvillian dynamics. *J. Stat. Phys.*, 68(5/6):673, 1992.
70. P. Gaspard. Diffusion in uniformly hyperbolic one-dimensional maps and appell polynomials. *Phys. Lett. A*, 168:13–17, 1992.
71. P. Gaspard. What is the role of chaotic scattering in irreversible processes? *Chaos*, 3(2):427, 1993.
72. P. Gaspard. Hydrodynamic modes as singular eigenstates of the Liouvillian dynamics: Deterministic diffusion. *Phys. Rev. E*, 53:4379–4401, 1996.
73. P. Gaspard. Entropy production in open volume-preserving systems. *J. Stat. Phys.*, 88:1215–1240, 1997.
74. P. Gaspard. *Chaos, scattering and statistical mechanics*. Cambridge University Press, Cambridge, 1998.
75. P. Gaspard. Scattering, transport and stochasticity in quantum systems. In J. Karkheck, editor, *Dynamics: Models and kinetic methods for non-equilibrium many body systems*, NATO ASI series. Kluwer, 2000.
76. P. Gaspard. Dynamical chaos and nonequilibrium statistical mechanics. *Int. J. Mod. Phys. B*, 15:209–235, 2001.
77. P. Gaspard. Diffusion and the Poincare-Birkhoff mapping of chaotic systems. In I. Antoniou, editor, *Dynamical systems and irreversibility*, volume 122 of *Adv. Chem. Phys.*, page 109, 2002.
78. P. Gaspard. Dynamical theory of relaxation in classical and quantum systems. In P. Garbaczewski and R. Olkiewicz, editors, *Dynamics of dissipation*, volume 597 of *LNP*, pages 111–163. Springer Verlag, 2002.

79. P. Gaspard, M. E. Briggs, M. K. Francis, J. V. Sengers, R. W. Gammons, J. R. Dorfman, and R. V. Calabrese. Experimental evidence for microscopic chaos. *Nature*, 394:865–868, 1998.

80. P. Gaspard, I. Claus, T. Gilbert, and J. R. Dorfman. Fractality of the hydrodynamic modes of diffusion. *Phys. Rev. Lett.*, 86(8):1506, 2001.

81. P. Gaspard and R. Klages. Chaotic and fractal properties of deterministic diffusion-reaction processes. *Chaos*, 8:409–423, 1998.

82. P. Gaspard and M. Nagaoka. Slippage of initial conditions for the Redfield master equation. *J. Chem. Phys.*, 111:5668–5675, 1999.

83. P. Gaspard and G. Nicolis. Transport properties, Lyapunov exponents, and entropy per unit time. *Phys. Rev. Lett.*, 65(14):1693, 1990.

84. P. Gaspard, G. Nicolis, and J. R. Dorfman. Diffusive Lorentz gases and multibaker maps are compatible with irreversible thermodynamics. *Physica A*, 323:294–322, May 2003.

85. P. Gaspard and S. A. Rice. Exact quantization of the scattering from a classical chaotic repeller. *J. Chem Phys.*, 90:2255, 1989.

86. P. Gaspard and S. A. Rice. Scattering from a classically chaotic repellor. *J. Chem. Phys.*, 90:2225–2241, 1989.

87. P. Gaspard and S. A. Rice. Semiclassical quantization of the scattering from a classically chaotic repellor. *J. Chem. Phys.*, 90:2242–2254, 1989.

88. T. Gilbert and J. R. Dorfman. Entropy production: From open volume-preserving to dissipative systems. *J. Stat. Phys.*, 96:225–269, 1999.

89. T. Gilbert, J. R. Dorfman, and P. Gaspard. Entropy production, fractals, and relaxation to equilibrium. *Phys. Rev. Lett.*, 85(8):1606, 2000.

90. T. Gilbert, J. R. Dorfman, and P. Gaspard. Fractal dimensions of the hydrodynamic modes of diffusion. *Nonlinearity*, 14:339–358, 2001.

91. S. Godoy and S. Fujita. A quantum random-walk model for tunneling diffusion in a 1d lattice - a quantum correction to fick law. *J. Chem. Phys.*, 97:5148–5154, 1992.

92. A. Goussev and J. R. Dorfman. Lyapunov spreading of semiclassical wave packets for the lorentz gas: Theory and applications. *Phys. Rev. E*, 71(2):026225, 2005.

93. G. Grimmett, S. Janson, and P. F. Scudo. Weak limits for quantum random walks. *Phys. Rev. E*, 69(2):026119, 2004.

94. T. Guhr, A. Müller-Groeling, and H. A. Weidenmïler. Random-matrix theories in quantum physics: common concepts. *Phys. Rep.*, 299:189–425, 1998.

95. F. Haake. *Quantum Signatures of Chaos.* Springer Verlag, Berlin, New York, 2nd. edition, 2001.

96. F. Haake, M. Kuś, and R. Scharf. Classical and quantum chaos for a kicked top. *Z. Phys. B*, 65:381, 1987.

97. J. H. Hannay and M. V. Berry. Quantization of linear maps on a torus - Fresnel diffraction by a periodic grating. *Physica D*, 1:267, 1980.

98. J. H. Hannay, J. P. Keating, and A. M. O. Dealmeida. Optical realization of

the bakers transformation. *Nonlinearity*, 7:1327–1342, 1994.

99. H. H. Hasegawa and W. C. Saphir. Decaying eigenstates for simple chaotic systems. *Phys. Lett. A*, 161:471–476, 1992.

100. H. H. Hasegawa and W. C. Saphir. Unitarity and irreversibility in chaotic systems. *Phys. Rev. A*, 46:7401–7423, 1992.

101. M. Hillery, J. Bergou, and E. Feldman. Quantum walks based on an interferometric analogy. *Phys. Rev. A*, 68(3):032314, 2003.

102. W. G. Hoover. *Computational Statistical Mechanics*. Elsevier Science Publishers, Amsterdam, 1991.

103. E. Hopf. *Ergodentheorie*. J. Springer, Berlin, 1937.

104. Y. Imry. *Introduction to mesoscopic physics*. Oxford University Press, Oxford, 1997.

105. N. Inui, Y. Konishi, and N. Konno. Localization of two-dimensional quantum walks. *Phys. Rev. A*, 69(5):052323, 2004.

106. P. Jacquod, I. Adagideli, and C. W. J. Beenakker. Decay of the loschmidt echo for quantum states with sub-planckscale structures. *Phys. Rev. Lett.*, 89:154103, 2002.

107. P. Jacquod, P. G. Silvestrov, and C. W. J. Beenakker. Golden rule decay versus lyapunov decay of the quantum loschmidt echo. *Phys. Rev. E*, 64:055203, 2001.

108. V. Jaksic and C. A. Pillet. Spectral theory of thermal relaxation. *J. Math. Phys.*, 38:1757–1780, 1997.

109. R. A. Jalabert and H. M. Pastawski. Environment-independent decoherence rate in classically chaotic systems. *Phys. Rev. Lett.*, 86:2490–2493, 2001.

110. C. Jarzynski. Nonequilibrium equality for free energy differences. *Phys. Rev. Lett.*, 78:2690–2693, 1997.

111. C. Jarzynski. What is the microscopic response of a system driven far from equilibrium? In P. Garbaczewski and R. Olkiewicz, editors, *Dynamics of dissipation*, volume 597 of *LNP*, pages 63–82. Springer Verlag, 2002.

112. C. Jarzynski and D. K. Wójcik. Classical and quantum fluctuation theorems for heat exchange. *Phys. Rev. Lett.*, 92:230602, 2004.

113. H. Jeong, M. Paternostro, and M. S. Kim. Simulation of quantum random walks using the interference of a classical field. *Phys. Rev. A*, 69(1):012310, 2004.

114. Kadanoff, L. P., and T. C. Escape from strange repellers. *Proc. Natl. Acad. Sci. USA*, 81:1276, 1984.

115. H. Kantz and P. Grassberger. Repellers, semi-attractors, and long-lived chaotic transients. *Physica D*, 17:75–86, 1985.

116. J. Kempe. Quantum random walks: an introductory overview. *Cont. Phys.*, 44(4):307–327, 2003.

117. V. Kendon and B. C. Sanders. Complementarity and quantum walks. *Phys. Rev. A*, 71(2):022307, 2005.

118. V. Kendon and B. Tregenna. Decoherence can be useful in quantum walks. *Phys. Rev. A*, 67(4):042315, 2003.

119. M. Khodas and S. Fishman. Relaxation and diffusion for the kicked rotor. *Phys. Rev. Lett.*, 84:2837–2840, 2000.

120. R. Klages. Microscopic chaos, fractals, and transport in nonequilibrium steady states, 2004. habilitation theses, TU Dresden.

121. R. Klages, P. Gaspard, H. van Beijeren, and J. R. Dorfman, editors. *Microscopic chaos and transport in many-particle systems*, volume 187 of *Physica D*. Elsevier, 2004.

122. P. L. Knight, E. Roldan, and J. E. Sipe. Quantum walk on the line as an interference phenomenon. *Phys. Rev. A*, 68(2):020301, 2003.

123. N. Konno, K. Mistuda, I. Soshi, and H. J. Yoo. Quantum walks and reversible cellular automata. *Phys. Let. A*, 330(6):408–417, 2004.

124. N. Konno, T. Namiki, T. Soshi, and A. Sudbury. Absorption problems for quantum walks in one dimension. *J. Phys. A*, 36(1):241–253, 2003.

125. M. D. Kostin. Cellular automata for quantum systems. *J. Phys. A*, 26:L209–L215, 1993.

126. J. Košík. Two models of quantum random walk. *C. Eur. J. Phys. (CEJP)*, 4:556, 2003.

127. J. Košík and V. Bužek. Scattering model for quantum random walks on a hypercube. *Phys. Rev. A*, 71(1):012306, 2005.

128. R. d. L. Krönnig, , and W. G. Penney. Quantum mechanics of electrons in crystal lattices. *Proc. R. Soc. London A*, 130:499–513, 1931.

129. R. Kubo, M. Toda, and N. Hashitsume. *Statistical Physics II. Nonequilibrium statistical mechanics.* Springer-Verlag, 1985.

130. J. Kurchan. Fluctuation theorem for stochastic dynamics. *J. Phys. A-Math. Gen.*, 31:3719–3729, 1998.

131. M. Kuś, J. Mostowski, and F. Haake. Universality of eigenvector statistics of kicked tops of different symmetries. *J. Phys. A*, 21:L1073–L1077, 1988.

132. A. Lakshminarayan. On the quantum bakers map and its unusual traces. *Ann. Phys.*, 239:272–295, 1995.

133. J. L. Lebowitz and H. Spohn. A gallavotti-cohen-type symmetry in the large deviation functional for stochastic dynamics. *J. Stat. Phys.*, 95:333–365, 1999.

134. V. Leonov. title? *Theor. Probability Appl.*, 6:87, 1961.

135. J. Liphardt, S. Dumont, S. Smith, I. Tinoco, and C. Bustamante. Equilibrium information from nonequilibrium measurements in an experimental test of jarzynski's equality. *Science*, 296:1832–1835, 2002.

136. C. C. Lopez and J. P. Paz. Phase-space approach to the study of decoherence in quantum walks. *Phys. Rev. A*, 68(5):052305, 2003.

137. W. T. T. Lu, K. Pance, P. Pradhan, and S. Sridhar. Quantum correlations and classical resonances in an open chaotic system. *Phys. Scr.*, T90:238–245, 2001.

138. T. D. Mackay, S. D. Bartlett, L. T. Stephenson, and B. C. Sanders. Quantum walks in higher dimensions. *J. Phys. A*, 35(12):2745–2753, 2002.

139. C. Maes. The fluctuation theorem as a gibbs property. *J. Stat. Phys.*, 95:367–

392, 1999.

140. L. Matyas, T. Tel, and J. Vollmer. Multibaker map for thermodynamic cross effects in dynamical systems. *Phys. Rev. E*, 62:349–365, 2000.

141. L. Matyas, T. Tel, and J. Vollmer. Thermodynamic cross effects from dynamical systems. *Phys. Rev. E*, 61:R3295–R3298, 2000.

142. L. Matyas, T. Tel, and J. Vollmer. Coarse-grained entropy and information dimension of dynamical systems: The driven lorentz gas. *Phys. Rev. E*, 69(1):016205, Jan. 2004.

143. B. Mehlig and K. Richter. Semiclassical linear response: far-infrared absorption in ballistic quantum systems. *Phys. Rev. Lett.*, 80(9):1936–1939, 1998.

144. M. L. Mehta. *Random matrices*. Academic Press, New York, 1991.

145. D. A. Meyer. From quantum cellular automata to quantum lattice gases. *J. Stat. Phys.*, 85:551–574, 1996.

146. G. P. Morriss and C. P. Dettmann. Thermostats: Analysis and application. *Chaos*, 8(2):321–336, 1998.

147. O. Mulken and A. Blumen. Slow transport by continuous time quantum walks. *Phys. Rev. E*, 71(1):016101, 2005.

148. O. Mulken and A. Blumen. Spacetime structures of continuous-time quantum walks. *Phys. Rev. E*, 71(3):036128, 2005.

149. A. Nayak and A. Vishwanath. Quantum walk on the line. quant-ph/0010117, 2000.

150. R. Newton. Comment on an article by sprung, wu and martorell ajp 61, 1118. *Am. J. Phys.*, 62:1042, 1994.

151. M. A. Nielsen and I. L. Chuang. *Quantum computation and quantum information*. Cambridge University Press, Cambridge, 2000.

152. P. W. Oconnor and S. Tomsovic. The unusual nature of the quantum baker transformation. *Ann. Phys.*, 207:218–264, 1991.

153. T. Oka, N. Konno, R. Arita, and H. Aoki. Breakdown of an electric-field driven system: A mapping to a quantum walk. *Phys. Rev. Let.*, 94(10):100602, 2005.

154. E. Ott. *Chaos in Dynamical Systems*. University Press, Cambridge, 1993.

155. K. Pance, W. T. Lu, and S. Sridhar. Quantum fingerprints of classical ruelle-pollicott resonances. *Phys. Rev. Lett.*, 85:2737–2740, 2000.

156. A. Patel, K. S. Raghunathan, and P. Rungta. Quantum random walks do not need a coin toss. *Phys. Rev. A*, 71(3):032347, 2005.

157. A. Peres. Stability of quantum motion in chaotic and regular systems. *Phys. Rev. A*, 30:2490, 1984.

158. M. Pollicott. On the rate of mixing of axiom a flows. *Inent. math.*, 81:413–426, 1985.

159. M. Pollicott. Meromorphic extensions of generalized zeta functions. *Inent. math.*, 85:147–164, 1986.

160. J. Preskill. Lecture notes for the course 'information for physics 219/computer science 219, quantum computation'. www.theory.caltech.edu/people/preskill/ph229, 1999.

161. T. Prosen. Ruelle resonances in kicked quantum spin chain. *Physica D*, 187:244–252, 2004.
162. T. Prosen, T. H. Seligman, and M. Znidaric. Theory of quantum loschmidt echoes. *Prog. Th. Phys. Sup.*, 150(150):200–228, 2003.
163. J. Rammer. *Quantum transport theory.* Perseus Books, 1998.
164. L. Reichl. *The Transition to Chaos: Conservative Classical Systems and Quantum Manifestations.* Springer-Verlag, New York, 2004.
165. P. Ribeiro, P. Milman, and R. Mosseri. Aperiodic quantum random walks. *Phys. Rev. Let.*, 93(19):190503, 2004.
166. F. Ritort. Work fluctuations and transient violations of the second law: perspectives in theory and experiment. *Sem. Poinc.*, 2:63–87, 2003.
167. A. Romanelli, R. Siri, G. Abal, A. Auyuanet, and R. Donangelo. Decoherence in the quantum walk on the line. *Physica A*, 347:137–152, 2005.
168. L. Rondoni. Deterministic thermostats and fluctuation relations. In P. Garbaczewski and R. Olkiewicz, editors, *Dynamics of dissipation*, volume 597 of *LNP*, pages 35–61. Springer Verlag, 2002.
169. L. Rondoni and E. G. D. Cohen. Gibbs entropy and irreversible thermodynamics. *Nonlinearity*, 13(6):1905–1924, Nov. 2000.
170. L. Rondoni, T. Tel, and J. Vollmer. Fluctuation theorems for entropy production in open systems. *Phys. Rev. E*, 61:R4679–R4682, 2000.
171. D. Ruelle. Locating resonances for axiom A dynamical systems. *J. Stat. Phys.*, 44:281, 1986.
172. D. Ruelle. Resonances of chaotic dynamical systems. *Phys. Rev. Lett.*, 56:405–407, 1986.
173. D. Ruelle. Resonances for axiom-a flows. *J. Differ. Geom.*, 25:99–116, 1987.
174. D. Ruelle. Smooth dynamics and new theoretical ideas in nonequilibrium statistical mechanics. *J. Stat. Phys.*, 95:393–468, 1999.
175. B. C. Sanders, S. D. Bartlett, B. Tregenna, and P. L. Knight. Quantum quincunx in cavity quantum electrodynamics. *Phys. Rev. A*, 67(4):042305, 2003.
176. M. Saraceno. Classical structures in the quantized baker transformation. *Ann. Phys.*, 199:37–60, 1990.
177. M. Saraceno and A. Voros. Towards a semiclassical theory of the quantum bakers map. *Physica D*, 79:206–268, 1994.
178. S. S. Schweber. Feynman and the visualization of space-time processes. *Rev. Mod. Phys.*, 58:449–508, 1986.
179. D. Shapira, O. Biham, A. J. Bracken, and M. Hackett. One-dimensional quantum walk with unitary noise. *Phys. Rev. A*, 68(6):062315, 2003.
180. N. Shenvi, J. Kempe, and K. B. Whaley. Quantum random-walk search algorithm. *Phys. Rev. A*, 67(5):052307, May 2003.
181. Y. G. Sinai. Dynamical systems with elastic reflections: Ergodic properties of dispersing billiards. *Russ. Math. Surv.*, 25(2):137, 1970.
182. D. W. L. Sprung, H. Wu, and J. Martorell. Scattering by a finite periodic

potential. *Am. J. Phys.*, 61:1118, 1993.

183. H. J. Stöckmann. *Quantum Chaos. An Introduction.* Cambridge University Press, Cambridge, 1999.

184. S. Succi and R. Benzi. Lattice boltzmann equation for quantum mechanics. *Physica D*, 69:327–332, 1993.

185. D. Szász, editor. *Hard Ball Systems and the Lorentz Gas*, volume 101 of *Encyclopaedia of mathematical sciences.* Springer Verlag, Berlin, 2000.

186. S. Tasaki. Irreversibility in reversible multibaker maps — transport and fractal distributions. In I. Antoniou, editor, *Dynamical systems and irreversibility*, volume 122 of *Adv. Chem. Phys.*, page 77, 2002.

187. S. Tasaki and P. Gaspard. Fick's law and fractality of nonequilibrium stationary states in a reversible multibaker map. *J. Stat. Phys.*, 81(5/6):935–987, 1995.

188. S. Tasaki and P. Gaspard. Thermodynamic behavior of an area-preserving multibaker map with energy. *Theor. Chem. Acc.*, 102:385–396, 1999.

189. S. Tasaki and P. Gaspard. Entropy production and transports in a conservative multibaker map with energy. *J. Stat. Phys.*, 101:125–144, 2000.

190. T. Tél. Transient chaos. In H. Bai-Lin, editor, *Directions in Chaos*, volume 3, pages 149–211. World Scientific, 1990.

191. T. Tél and J. Vollmer. Entropy balance, multibaker maps, and the dynamics of the Lorentz gas. In D. Szász, editor, *Hard Ball Systems and the Lorentz Gas*, volume 101 of *Encyclopaedia of Mathematical Sciences*, pages 369–418. Springer Verlag, Berlin, 2000.

192. T. Tel, J. Vollmer, and W. Breymann. Transient chaos: The origin of transport in driven systems. *Europhys. Lett.*, 35:659–664, 1996.

193. T. Tel, J. Vollmer, and L. Matyas. Comments on the paper 'particles, maps and irreversible thermodynamics' by e.g.d. cohen, l. rondoni, physica a 306 (2002) 117. *Physica A*, 323:323–326, May 2003.

194. P. Törma. Transitions in quantum networks. *Phys. Rev. Lett.*, 81:2185–2189, 1998.

195. B. C. Travaglione and G. J. Milburn. Implementing the quantum random walk. *Phys. Rev. A*, 65:art. no.–032310, 2002.

196. L. Van Hove. Correlations in space and time and born approximation scattering in systems of interacting particles. *Phys. Rev.*, 95:249, 1954.

197. J. Vollmer. Chaos, spatial extension, transport, and non-equilibrium thermodynamics. *Phys. Rep.*, 372(2):131–267, 2002.

198. J. Vollmer, T. Tel, and W. Breymann. Equivalence of irreversible entropy production in driven systems: An elementary chaotic map approach. *Phys. Rev. Lett.*, 79:2759–2762, 1997.

199. J. Vollmer, T. Tel, and W. Breymann. Entropy balance in the presence of drift and diffusion currents: An elementary chaotic map approach. *Phys. Rev. E*, 58:1672–1684, 1998.

200. J. Vollmer, T. Tél, and W. Breymann. Dynamical-system models of transport:

chaos, characteristics, the macroscopic limit, and irreversibility. *Physica D*, 187:108–127, 2004.

201. J. Vollmer, T. Tel, and L. Matyas. Modeling thermostating, entropy currents, and cross effects by dynamical systems. *J. Stat. Phys.*, 101:79–105, 2000.

202. G. M. Wang, E. M. Sevick, E. Mittag, D. J. Searles, and D. J. Evans. Experimental demonstration of violations of the second law of thermodynamics for small systems and short time scales. *Phys. Rev. Let.*, 89:050601, 2002.

203. J. Weber, F. Haake, and P. Seba. Frobenius-perron resonances for maps with a mixed phase space. *Phys. Rev. Lett.*, 85:3620–3623, 2000.

204. M. Wilkinson. A semiclassical sum rule for matrix elements of classically chaotic systems. *J. Phys. A-Math. Gen.*, 20:2415, 1987.

205. D. A. Wisniacki, E. G. Vergini, H. M. Pastawski, and F. M. Cucchietti. Sensitivity to perturbations in a quantum chaotic billiard. *Phys. Rev. E*, 65:055206, 2002.

206. A. Wojcik, T. Luczak, P. Kurzynski, A. Grudka, and M. Bednarska. Quasiperiodic dynamics of a quantum walk on the line. *Phys. Rev. Let.*, 93(18):180601, 2004.

207. D. Wójcik, I. Białynicki-Birula, and K. Życzkowski. Time evolution of quantum fractals. *Phys. Rev. Lett.*, 85(24):5022, 2000.

208. D. K. Wójcik and J. R. Dorfman. Quantum multibaker maps: Extreme quantum regime. *Phys. Rev. E*, 66:036110, 2002.

209. D. K. Wójcik and J. R. Dorfman. Diffusive-ballistic crossover in 1D quantum walks. *Phys. Rev. Lett.*, 90:230602, 2003.

210. D. K. Wójcik and J. R. Dorfman. Crossover from diffusive to ballistic transport in periodic quantum maps. *Physica D*, 187(1-4):223–243, 2004.

211. M. Wojtkowski. Principles for the design of billiards with nonvanishing Lyapunov exponents. *Comm. Math. Phys.*, 105:391–414, 1986.

212. M. Yamaguti, M. Hata, and J. Kigami. *Mathematics of Fractals*, volume 167 of *Mathematical Monographs*. American Mathematical Society, Providence, Rhode Island, 1997.

213. R. Zwanzig. *Nonequilibrium statistical mechanics*. Oxford University Press, 2001.